INSTRUCTIONS to AUTHERS

Submitted articles to the Journal of Madinat Al-Elem University College can be published in all fields related to the Academic Departments of the College (Biology, Law, programming Engineering Sciences, Computer Techniques Engineering Law, Medical Physics, Civil Engineering, and Accounting).

Written request for publication and signing a consent form to publish must be for articles which have not been published or submitted for publication to other journals. Three copies with CD are needed. Manuscripts should be typed on: A4 white paper, double spaced, written in Times New Roman font size 14. Margins should be 3cm from top, bottom, left and right. The main title should be in: bold Times New Roman font size 14. Author names should be written in the following sequence: first name, middle name, the family name, followed by the names of departments and institutions of work. A footnote accompanies the first page stating the full address of correspondence author.

Articles need to contain the following items:
- Abstract in English and Arabic not more than 300 words.
- Article includes the following items: Introduction, Materials and Methods, Results and Discussion, Conclusion and References.
- References should be numbered in the text according to the sequence appeared in the text and listed in order.
- Tables and figures should be appropriately titled with size not exceed an A4 page.

The editor reserves the right to reject or accept any article submitted.

Publication charges: Each accepted paper is required to pay the publication charge (100,000 Iraqi dinars). Five thousands Iraqi dinar are requested for each extra page extra printed page.

Contents

Multimedia Steganography Based on Least Significant Bit (LSB) and Duffing map

Jinan N. Shehab[1], HaraaRaheemHatem [2]

[1, 2]Communication Department, College of Engineering, University of Diyala

ABSTRACT

This paper presents hiding the text or image (secret information) inside other image (cover image) based on Least Significant Bits (LSB). The position of characters in original secret text and the position of pixels in original secret image have been changed by Duffing map (random number generator). The fundamental idea is to insert the secret message (text, gray image and color image) in the least significant bits of the cover image (gray or color image). This actually works because the Human Visual System (HVS) is not sensitive enough to pick out changes in color. The experiments and comparative studies show that the algorithms are characterized by many features of the ability of hiding huge data, and then the ability of extracting secret message without errors. Beside the return image, has efficacies (to human acquaintance) according to peak signal to noise ratio (PSNR) and mean square error (MSE), also retain both the explicitness and the characteristics of the both secret message and cover image.

Keyword: steganography, LSB algorithm, image steganography, text steganography, Duffing map.

اخفاء الوسائط المتعدده باستخدام البت الاقل وزنا في حسابات الارقام واستخدام مولد عشوائي للاعداد

جنان نصيف شهاب [1]،حراء رحيم حاتم [2]

[1،2]مدرس مساعد،   كلية الهندسه جامعة ديالى

الخلاصه:

يقدم هذا العمل اخفاء نص او صوره داخل صوره بالاعتماد على البت الاقل وزنا بعد تغيير مواقع الحروف في النص الاصلي ومواقع وحدات الصورة في الصوره المراد اخفائها باستخدام المولد العشوائي للاعداد (Duffing map).

الفكره الاساسيه في هذا العمل هو ادخال النص او الصوره (الملونه, الرماديه) في البتات الاقل وزنا في الصوره الاصليه (الملونه, الرماديه). يعتبر هذا العمل حقيقي لان العين البشريه لاتتحسس التغييرات الطفيفه في الالوان. لقد بينت التجارب والدراسات ان الخوارزميات المستخدمه تتحدد صفاتها عن طريق قابليتها في اخفاء عدد كبير من البيانات وعن طريق قدرتها في استرجاع الرساله الاصليه بدون اخطاء.

أمتلكت الصورةالمسترجعهكفاءةاتعالية (إلبالتعارفالبشري) بالاعتماد على نسبةالضوضاء (PSNR) ومعدلمربعالخطأ (MSE). ان البرنامج المقترح وفر حماية عاليه للنص والصورة السرية لحاجة المسترجع الى المفتاح الاصلي وفي حالة حدوث تغير بسيط في المفتاح فستنعدم فرصة استرجاع المعلومات الاصلية. لقد تم انجازالبحث باستخداملغة MATLAB.

Introduction

The development of computer and expanding its use in different areas of life and work, the issue of information security has become increasingly important, security becomes increasingly important for many applications. One of the grounds discussed in information security is the exchange of information through the cover media, for that; different methods such as, steganography, coding, watermarking … etc have been used to improve image security [1].

Steganography is the art of secret communication or the science of invisible communication. It is nothing more mechanism to conceal message (secret object) inside anther innoxious message (cover object) in a way that nobody except the recipient (who must know the technique used) can detect there is a second (secret) message present [2].In the face of, there are many different carrier file format (cover) can be used but digital image are the most popular because hold large amount of data and their frequency on the internet [3].

In this paper, will take one of the methods of steganography it is LSB, it's used to hide text in image and gray image in cover image.To add more security, the data to be hidden is permutated with a key created by Duffing map and then the new shuffling message is embedding into cover image. To extract the hidden information, one should have the same key using in the transmitter to extract the message. This work includes two algorithms; hiding text in an image (gray-scale plus color image) and hiding gray-image in an image (gray-scale plus color image).In these algorithms, interest has been expressed to the quality of the extracted secret information (reconstructed message quality) beside the quality of the stego-image, compared with the original cover.

1- Least Significant Bit (LSB) substitution method

The LSB is a very popular way of embedding secret messages with simplicity. The fundamental idea here is to insert the secret message in the least significant bits of the cover images. This actually works because the human visual system is not sensitive enough to pick out changes in color (whether gray or color) and digital covers have a large number of redundant bits.

A basic algorithm for **LSB** substitution is to take the first N cover pixels where N is the total length of the secret message (for text and image where (N=R×C where R row and C column numbers in secret image))that is to be embedded in bits. After that every pixel's last bit in cover image will be replaced by one of the message bits [4,5].

2- Duffing Map (also called as Holmes map)

A two-dimensional discrete-time nonlinear dynamical system was proposed by German electrical engineer Georg Duffing [6].   As a simplified model of the Poincare map for the Duffing map module is given by:-

$$X_{n+1} = Y_n$$
$$Y_{n+1} = -bX_n + aY_n - Y_n^3$$

(1)

The map depends on the two constants or parameters *a* and *b,* this map is shown in Figure1. The diagram is a strange attractor popularly known as the Duffing attractor.

4- The Steganography System Procedure

First in these systems, the cover image should be selected carefully like choosing the cover with low details (as shown in Figure 2, cover image with low details all have the same size 512×512) so when the information in the pixels is replaced with another information, the cover image will not have a noticeable degradation. In this work, the procedure of steganography divided in two sides:

4-1 Embedded Side

Figure 3 shows the stages involved in the sending process. Each stage will be briefly discussed below:

Step 1.Preparation of The Cover Image: Transform 2-D image (R×C) into 1-D image (N).

Step 2.Preparation of The Secret Message: In this algorithm, a secret text is being reading and then transform each character into equivalent number according to the American Standard Code for Information Interchange (ASCII). From other side the secret image transform from 2-D into 1-D.

Step 3.Shuffling by Duffing Map: this contain many sub-steps;

Set the key (initial conditions X(0)= 0.1, Y(0)=0.003 and parameters a=2.75, b=0.15) in acceptable intervals to generate random number. the real value result from Duffing map is modified to integer value between (0,255) [6].

$$X_D(n) = mod(floor(X_H(n) \times 10^{15}), 256)$$
$$Y_D(n) = mod(floor(Y_H(n) \times 10^{15}), 256)$$

(2)

1. Conduct the function "Sort" on X_D and Y_D for constructing scrambling index array I_1 and I_2 with dimension (same dimension of the secret text or image)arranged in ascending order.

2. Rearrangement of the decimal value onsecret message according to the sort of the random key as shown in the Figure (4).

Step 4. Proposed Embedding Algorithms

A. Hiding Text in an Image:-In this algorithm, a secret text message is embedded in a cover image, as shown in Figure(3-A) . The algorithms step represented by:

1- After shuffling text, transform each decimal value into binary number (8-bits/numbers).

2- Convert the cover image into binary number (if gray image (8-bits/pixel)and (24-bits /pixels) if color image is used).

3- Replace the value of last bit in every pixel (in cover image) by the value of bit from secret text, then every pixel's last bit in cover image will be replaced by one of the message bits. As show in algorithm and Table 1.

4- Transform results back from binary to decimal to get stego-image

B. Hiding Image in an Image: In this algorithm, a secret image will be hidden in a cover image as shown in Figure(3-B).The steps for this algorithms are:

1- After shuffle secret image by using Duffing map. Each pixel in secret image represented by (8-bits/pixel (gray-image)).

2- Hidden each bit from secret image in the last bit from each pixel in cover image according to LSB algorithm.

3- Transform back from binary to decimal and then from 1-D to 2-D to get stego image.

4-2 Reconstructed Side

To extract the secret information, the receiver need stego-image and the secret key (initial conditions (X(0) , Y(0)) and parameters (a,b)) of Duffing map . The extracting algorithm is the inverse of the embedding algorithms , as shown in Figure (5):

   A- Extract Text from Image

As in extracting text from image as shown in Figure (5-A) ,the same steps will be followed:-
1. Convert the steg image from 2-D into 1-D and then convert each pixel to binary number (8-bit/pixel).

2. Take the last bit from each pixel to construct the secret text (binary)

3. Transform from binary to decimal value.

4. Return the value to their original position depending on initial condition (X(0) and Y(0)) and parameters (a,b) from Duffing map.

5. After return every value to its position transforms each value into character according to ASCII.

B- Extracting Image from Image

Figure 5-B shows that this process will be done by following steps:

1. Convert the steg image from 2-D into 1-D and then convert each pixel to binary number (8-bit/pixel).

2. Take the last bit from each pixel to construct the secret image (binary)

3. Transform from binary to decimal value.

4. Return each pixel to its original position the value depending on initial condition (X(0) and Y(0)) and parameters (a,b) from Duffing map.

5. After return every value to its position transform from 1-D into2-D to construct secret image.

5-Numerical Simulation Results

There are many tests that can be used to measure the quality and security of the image:-

5-1 Peak-Signal-to-Noise-Ratio (PSNR)

According to the Human Visual System (HVS), some amount of distortion between the original image and the modified one is allowed. The **P**eak **S**ignal-to-**N**oise **R**atio known as **PSNR** is used as the scale for image quality (which computes the peak signal-to-noise ratio) between the original image and stego image [7]. PSNR is usually measured in dB. To compute the peak signal to noise ratio, then:-

$$PSNR(dB) = 10log_{10}\frac{P^2}{MSE} \qquad (3)$$

Where;**P** is the maximum pixel value. Also, the   Mean Square Error (**MSE)** which measures the cumulative **M**ean **S**quare **E**rror between the original and the stego image. The **MSE** is defined

$$MSE = \frac{1}{R \times C}\sum_{i=0}^{R-1}\sum_{j=0}^{C-1}[X(i,j) - \hat{X}(i,j)]^2 \qquad (4)$$

as:

Where*: R*: number of pixel in rows, *C*: number of pixel in columns, *i and j* : row and column numbers, X(i,j): original image and $\hat{X}$(i,j): stego image.

By using Matlab program, the simulation result for the proposed method are:-

1. Hiding a text into a gray image also hiding text in color image. The implementation results to hide three different text size and result of PSNR (between original image and Stego-image) for both in gray and color image are shown in Table(2).

2. Hiding a gray image into a gray image and a gray image into a color image and then color image into color image. The implementation results can be seen in Table (3).

From Tables 2,3 &4, the result of PSNR for using color image as cover are higher compare with gray image as cover image. The size of the color image is larger than the size of the gray image that is the problem, for that gray image has been used as cover image in this paper. Also we noted that PSNR is reduced when secret information (text or image) size increased because of more pixel in cover image is changed (more noise).

6- Histogram Analysis

The histogram of the cover image and the stego-image are found to show that the statistical properties of the cover image are not affected by changing one bit in some pixels [2]. Therefore, if the histogram of the cover is nearly equal to the histogram of the steg- image, this means that the proposed system is good enough to avoid the attackers. The three types of the images used in our algorithm. Figure 6 represented one example (Baby.jpg) of the cover and stego-images histograms, we noted that histogram of image before hiding information is the same that after hiding information because of the small change in some pixels don't effect on the histogram of the cove image as shown in Figure 6.

7- Key Space Analysis

Key space size is the total number of different keys that are used in the encoding .Here , the possible key size is 10^{30} keys for system . Exhaustive key search will take 2^d operations to succeed, where d is the key size in bits [2]. Any attacker simply tries all keys, one by one, and checks whether the given secret image. Therefore, the combinations of the parameters and initial conditions are large enough to prevent such exhaustive search.

7-1 Key Sensitivity Test

The key sensitivity is the degree of the changes in the encoding image caused by a tiny change in secret key [7,8], as shown in Figure (7).From this test the proposed algorithm is very sensitivity to tiny change in key=10^{-15}, then only by using the exact key can return the original secret message.

8-Conclusion

The simulation results show that, the proposed algorithm has high HVS for extracted secret message, also the stego-image is obtained with very close properties to the original cover image according to PSNR, MSE, HVS, and histogram tests, so it is so difficult to distinguish between

them. Using Duffing map to encoding secret message gives large enough key space $=10^{30}$ and very sensitive to the secret keys.

REFERENCES

[1]   ShashikalaChannalli And   Ajay Jadhav, "Steganography An Art Of Hiding Data", Sinhgad College Of Engineering, Pune,ShashikalaChannalli Et Al /International Journal On Computer Science And Engineering Vol.1(3), 137-141,2009.

[2]   ZaynabNajeebAbdulhameed,"High Capacity Steganography Based On Chaos And Contourlet Transform For Hiding Multimedia Data",M.Sc. Thesis, Department of Electronics & CommunicationsEngineering ,University of AL-Mustansiriy2014.

[3]   Morkel , Eloff , Olivier" An Overview Of Image Steganography" Information and Computer Security Architecture (ICSA) Research Group Department of Computer Science, University of Pretoria, Pretoria, South Africa,2005.

[4]   FahimIrfanAlam "An Investigation into Encrypted Message Hiding Through Images Using LSB", International Journal of Engineering Science and Technology (IJEST), 2011.

[5]   Bhavana.S, and K.L.Sudha" Text Steganography Using LsbInsertion Method Along With Chaos Theory", International Journal of Computer Science, Engineering and Applications (IJCSEA) Vol.2, No.2, April 2012.

[6]   Jing Xia, SuwenZheng, BaohongLv, CaihongShan"Harmonic Solutions of Duffing Equation with Singularity via Time Map", Applied Mathematics, 2014, 5,1528-1534.

[7]   Shreenandan Kumar, SumanKumari, SuchetaPatro, TusharShandilya and Anuja Kumar Acharya"Image Steganography using Index based Chaotic Mapping", International Conference on Distributed Computing and Internet Technology (ICDCIT), 2015.

[8]   Rosanne English," Comparison of High Capacity Steganography Techniques", IEEE , International Conference of Soft Computing and Pattern Recognition, 978-1-4244-7896-2,2010,(IVSL).
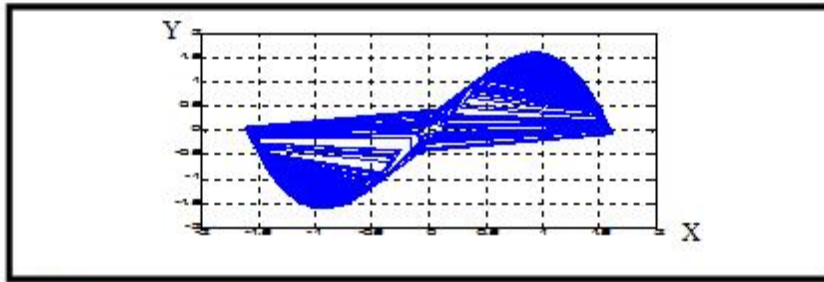
Figure (1) Duffing map attractor.

Little girl.jpg(512×512)   Chicken.jpg(512×512)   Baby.jpg(512×512)
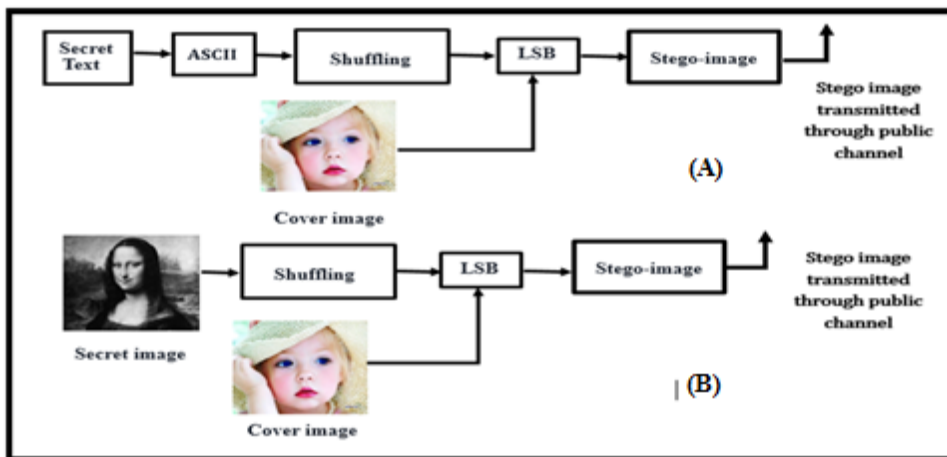
Figure (2) cover images.

Figure (3) proposed of embedded system.

A: embedded system for Text.

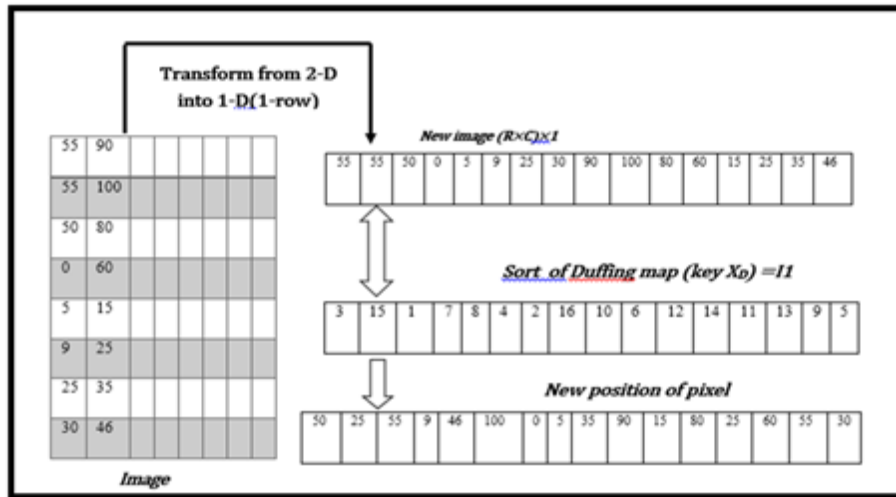B: embedded system for gray level image.
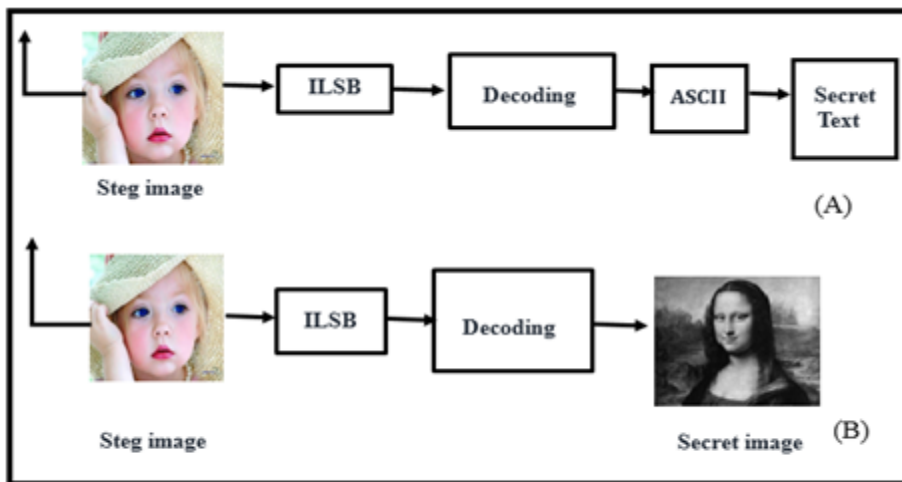
Figure (4) Pixel Shuffling inside Each Block.

Figure (5) proposed of extract system.

A: extracted system for Text.

(A) Original image	Decoding by the original key	Decoding by the neighbor key
	$X_D(0) = (0.1)$	$\hat{X}_D(0) = (0.000000000000001) = 10^{-15}$

B: extracted system for gray level image.
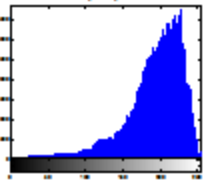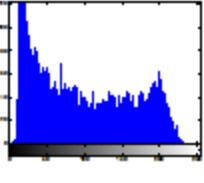
13

University of Diyala/ College of Engineering/ Communications Department/ paper title(Multimedia Steganography Based on Least Significant Bit)	University of Diyala/ College of Engineering/ Communications Department/ paper title(Multimedia Steganography Based on Least Significant Bit)	tynttderiaelSlen rtDanSosm nttrgmee(cdoatinLeinaeegafigf siM nil)Cioa/no aCeoaoipntapocvryEheDtseuuem / irigm Bi/i pf ieUty paitaBnlgngls

Image	Histogram	Secret image	Histogram
Cover image	Befor hiding information	Before stego	Before embedding
Stego-image	After hiding information	After reconstruction	After reconstruction

Figure (6) Cover and Stego -Images Histograms.

Cover image	Secret image	Stego-image	Extraction Secret image	PSNR
				56.3197
				61.1079
				56.3367

Figure (7) Sensitivity Tests of Keys A) Original Image B) Decoding Image by Using Original Key and C) Decoding Image by Using Neighbored Key.

Table (1) Embedding Steps (Replaced Last Bit in Every Pixel by Bit from Secret Message).

Data	Decimal value(ASCII)	Binary transform		
Secret message (as letter (A))	65	0 1 0 0 0 0 0 1		
Cover image (gray-scale)	(7-pixel in 1-row)	Binary transform	Embedding steps	Number of changing bits
	1. P1=241	1. 11110001	1. 11110001	3-bits in 8-pixels to hide one character (8-bits)
	2. P2=241	2. 11110001	2. 11110000	
	3. P3= 239	3. 11101111	3. 11101110	
	4. P4=237	4. 11101101	4. 11101100	
	5. P5=234	5. 11101010	5. 11101010	
	6. P6=230	6. 11100110	6. 11100110	
	7. P7=227	7. 11100011	7. 11100011	
	8. P8= 224	8. 11100000	8. 11100000	

Table (2) Hiding Text in Image and PSNR to each State.

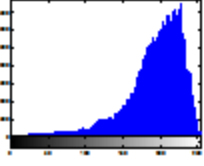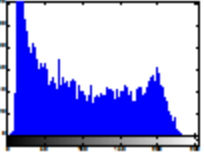| Text	PSNR(*girl*)			
	Gray image	Color image	Gray Stego- image	Color Stego-image
Red	92.8078	97.121	PSNR=75.8848	PSNR=80.1404
Communication Department	83.9617	87.9367		
University of Diyala/ College of Engineering/ Communications Department/ paper title(Multimedia Steganography Based on Least Significant Bit)	75.8848	80.1404		

Table(3) Results of Hiding Image in Image also PSNR for Each State.

Table(4) PSNR for Different Size of Secret Image.

Size of Secret image	Image name (image size)					
	Little girl.jpg(512×512)		Chicken.jpg(512×512)		Baby.jpg(512×512)	
	PSNR(gray in gray image$\approx$ color in color image)	PSNR (gray in color)	PSNR(gray in gray image$\approx$ color in color image)	PSNR (color)	PSNR(gray in gray image$\approx$ color in color image)	PSNR (color)
50×50	62.3585	67.1441	62.3680	67.1353	62.3109	67.1379
100×100	56.3464	61.1036	56.3276	61.0907	56.3197	61.1079
150×150	52.8151	57.5705	52.8103	57.5844	52.8085	57.6048
200×200	50.4016	55.0618	50.4861	55.0774	50.3459	55.0841
250×250	48.2149	53.1297	48.2107	53.1449	48.2187	53.1468

Design and Implementation of Accurate Foot drop Prosthesis System

Abbas FadhalHumadi, LubanHamdyHameed, ZainabMajidNahy, Middel Technical University/ College of Electrical and Electronic Engineering Techniques. Baghdad-Iraq.

E-Mail: ahumadi@yahoo.com,drabbas1962@gmail.com.Luban_alqudsi@yahoo.com, zainabmajid@gamail.com.

Abstract:

In present study, an accurate foot drop prosthesis device is presented. The design of the proposed system depends on electrical stimulation generated by electronic stimulator within specific requirements. This train of pulses that delivered to the targeted group of muscles innervate by pearonal nerve, using adhesive surface electrodes, has effective voltage amplitude, duration and frequency to stimulate these muscles to lift the dropped foot of the ground effectively during the swing phase of the gait cycle. The operation begins when the patient start to walk, so starting of the swing phase will be sensed using pressure sensor located under the heel of the patient's dropped foot. In this case, the electronic stimulator will be activated by the pressure sensor to start sending the stimuli that activate the muscles to lift the dropped foot causing the gate to be balanced and normal. Results shows that the output wave form of the stimulator is biphasic type pulse wave of net charge close to zero, with maximum voltage amplitude of 90V, frequency of 62Hz, and duration of 600ms.The current delivered to the muscles will be dependent on the tissue impedance and the voltage assigned for stimulation. This output pulses will be comfortable to the patient and cause accurate effective stimulation to the targeted group of muscles, leads to cancel the effect of dropped foot.

Key words: Foot drop, Prosthesis System, Foot, Muscle.

تصميم وتنفيذ معينة سقوط القدم الدقيقة

م.د. عباس فضال حمادي, م.م. لبان حمدي حميد, م.م. زينب ماجد ناهي.

الجامعة التقنية الوسطى. كلية التقنيات الهندسية الكهربائية والالكترونية/قسم هندسة تقنيات الأجهزة الطبية.

الملخص

يردفيهذهالورقة، تقديمجهازمعينة سقوط القدم الدقيقة.
تصميمالنظامالمقترحيعتمدعلىالتحفيز الكهربائيالتيتمإنشاؤهبواسطةمحفزالكترونيضمن متطلباتمحددة. هذه النبضاتالتيجهزتإلىالمجموعةالمستهدفةمنالعضلاتوالمحفز ةبعصبالساق (Pearonal Nerve)، وذلك باستخدامأقطابالسطحاللاصقة، تكونذات

موجةجهدوفعالومدةوتواترلتحفيز هذهالعضلاتبرفعالقدمالمنخفضةعنالأرضبشكلفعالأثناءمرحلةدورةالمشي. حيثتبدأمرحلة دورةالمشي من خلالاستخدامجهاز استشعار الضغطالموجودتحتكعبالقدمالمنخفضةللمريض. فيحالة رفع القدم عن الارضسيتمتفعيلالدائرةالإلكترونيةبجهاز استشعار الضغطليبدإرسالالمحفزات الكهربائيةالتيتنشطالعضلاترفعالقدمالمنخفضةوبذلكتكون الخطواتمتوازنةوطبيعية. وقد بينتالنتائج،شكلموجةالإخراجللمحفز الالكترونيبيشكل موجة نبضيةثنائيةالطوراتصافي شحنةقريبةمنالصفر،معأقصى سعةجهدتصل الى 90فولت،وبتردد مقداره 62 هرتز،ومدة 600ملي ثانية. هذا التيار الخارجإلىالعضلاتسوفيعتمد علىمقاومةالأنسجةوالجهدالمخصصللتحفيز.
هذهالنبضاتالخارجةسوفتكونمريحةللمريضوتسببالتحفيز الفعالوالدقيقإلىالمجموعةالمستهدفةمنالعضلات،ويؤديإلىالإلغاءأثرس قوط القدم عند السير علىالأقدام.

الكلمات المفتاحية: سقوط القدم. نظام تحفيز . قدم. عضلة

Introduction

The problem of dropped foot can be defined as the foot drag on the ground during the gait cycle especially within the swing phase and the ankle is not properly flexed. This problem commonly observed after many health problems especially, stroke, injuries of spinal cord, and some central nervous system (CNS) disorders [1]. The foot drop described as inability to lift foot which leads to tripping or steppage gait, so the patient left their knee high during swing phase to prevent tripping over the hanging down foot and then at the beginning of the stance phase, the foot slaps the floor. The foot drop caused many changes to the patient gait which leads to decrease the safety and efficiency of the gate, mobility limitation, and unstable gait leads to increasing risks of falls during walking, balance problems and impaired mobility, so walking becomes harder [2, 3]. Foot drop treated traditionally by using ankle foot orthosis (AFO), which is typicallya polyethylene brace that wraps under the foot and behind the calf to prevent the foot from dragging on theground. AFOs are characterized by simplicity and low priced, so it has good popularity,but also have a number of significant drawbacks and limitations; therefore, researchers have developedanther ways to treat foot drop, so functional electrical stimulation (FES) have been developed [2,4]. FES is defined in general as an artificial electrical stimulation of a muscle that has lacked of neural control, to provide muscle control to produce movement as normal movement and to restore functions lost after the impairment of nervous system. In this method, a train of short electric pulses are used to stimulate the motor neurons of the impaired organ to perform the contraction of targeted muscle. All kind of organs that has skeletal muscles with impairment could be make use of FES, so typical applications of FES system include treatment of the problem of dropped foot by stimulating common peroneal nerve to make contraction of the ankle dorsiflexors, enabling lower-limb paraplegics to stand or sit, and recover the function of hand in the paralyzed upper limb [5,6]. FES devices used basically three types of electrodes to stimulate the motor neurons which are, surface electrode , needle, or implantedelectrodes [3]. FES can provide many benefits that AFO's can't provide or poorly provide it, like active muscle contraction, enhance the strength of muscle, muscle tone reduced, energy efficiently uses of muscles of the lower limb, helps with motor relearning. FES may be used to greatly enhance gait function for patients that survive stroke, who clinically fit the requirements and have the motivation to do ambulatory training with the device [7]. The first FES system used for treating foot drop was introduced by Liberson and others researchers, in which they used external stimulator activated by sensor that detects the start of the swing phase of the impaired leg of the stroke patient, to stimulate the common peroneal nerve using external electrodes to flex the ankle of the patient and make the foot lift from the ground during the swing phase [8]. Another approach presented by Cameron, The WalkAideFES System that stimulate the leg transcutaneously by stimulate the peroneal nerve using a cuff that placed blow the knee of the patient, it contains a tilt sensors, accelerometer and inclinometers to calculate the speed and position of the leg and used these information to activate the pulse generator to trigger the peroneal nerve in order to prevent foot from dropping [2]. The most recent approach for treatment of foot drop introduced by Shimada and other researchers. There method represented by using acceleration sensor placed on the thigh of the targeted leg to detect the swing phase depending on the acceleration speed of the targeted leg, using neural network technology, to stimulate the peroneal nerve and correct the position of the foot during the swing phase [9]. In this paper, an efficient FES system will be presented to easily and efficiently treat the foot drop of stroke patient. The main components of the proposed system are shown in Figure 1.
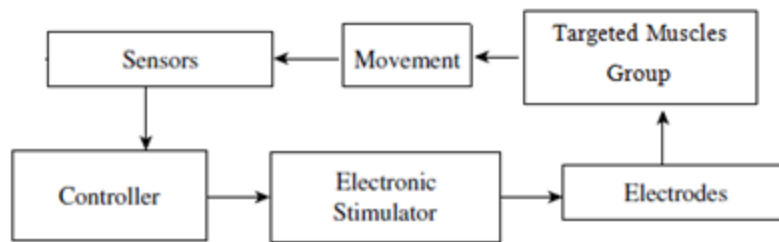
Figure 1. Main components of the proposed system

In which efficient and accurate stimulator will activated by a switch act as a sensor, this switch will be fitted under the dropped foot to work as a pressure sensor, it will tell the controller to activate the stimulator when the dropped foot has lifted from the ground, the stimulation will be conducted through surface electrode, which it is more easily accepted by patients, because it is noninvasive and no need for surgery to fit it on the target group of muscles.

System Design

The duration of the stimulus pulses, amplitude, output impedance of the generator, and impedance of electrodes, determine the electrical charge that will delivered to targeted muscles. These parameters are varies widely depending on the type of the stimulation, type of electrodes, its placement, its surface area, and the factor of safety used. In general, stimulation can be achieved using amplitude of asurface stimulation electrodeis less than 150V, and between 10 to 150 mA. The frequency of the stimulation is less than 100 Hz, and thepulse width is less than 1ms. these devices can work as a voltage regulated or current regulated device[6, 10,11]. The proposed stimulator electronic circuit is shown in figure (2) which is working as a voltage regulated stimulator, so the amount of voltage that make the best stimulation can be set by the patient manually once at the first time to use the device to reach the best results, and this will depend on the patient tissue impedance that specify the amount of current to be delivered to the muscle group.
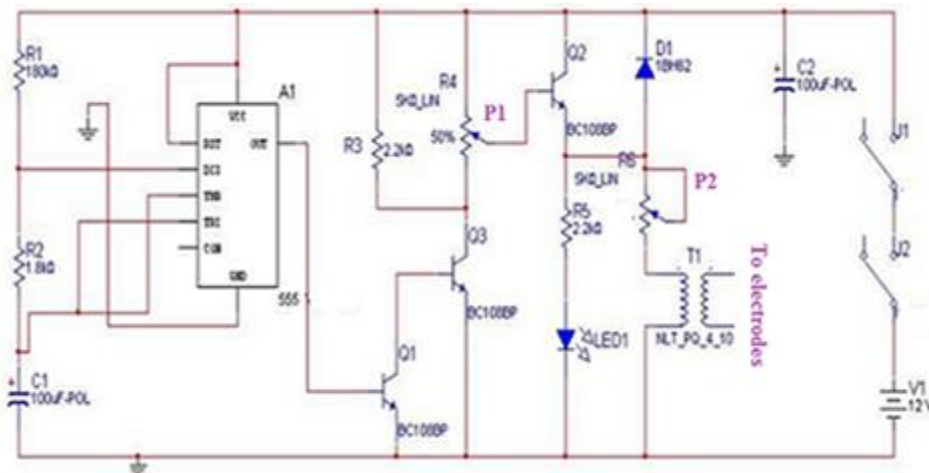

Figure 2. Stimulator proposed electronic circuit.

In the proposed design, the 555 IC will be the heart of the stimulator, in which by using suitable values for R1, R2 and C1, it will oscillate at a frequency of 62 Hz [12, 13]. These square waves with low frequency has low voltage amplitude, so it needed to be amplified to be suitable for triggering the targeted muscle group to be contracted, so the first stage of amplification will be done using PNP power transistors Q1 and Q3, this amplification factor will be adjusted used variable resistance (P2) to control the amplitude of the output pulse to be suitable for muscle stimulation. The diode that connected with emitter of Q2 and collector will protect the power transistor Q2 from inductive reactance that may lead to destroy it. The final stage of amplification will be done by using a step up transformer, so it will give the final amplification of the low frequency pulse generated by the 555 oscillator to be fitted with the requirements of muscle stimulation, the transformer will export a pulses of about 90 V maximum to the electrodes.These electrodes will be external type adhesive electrodes, which are easy to fit on the targeted muscle group; can be replaced at any time and low cost, so it is user friendly electrodes.The stimulator will be activated using switch J1, which it is a pressure sensor fitted under the heel of the dropped foot. It will sense the placement of the dropped foot on the ground during the stance phase, so when the patient lift his dropped foot at the start of the swing phase, the sensor will sense lose of pressure and activate the stimulator to stimulate the contraction of muscles to lift the dropped foot via the electrodes. The other switch is the ON/OFF switch.The power source used is a small 12 V Heavy duty type battery, to easily provide the system with the required power for a long time without increasing largely the weight of the device, and can be replaced anytime easily.   The proposed system is shown in figure (3), (4) and (5).
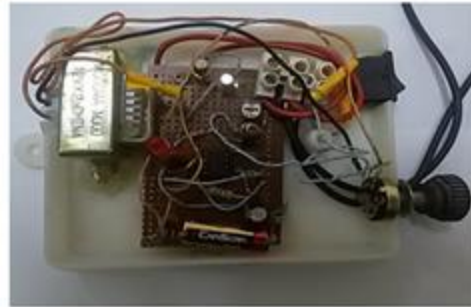
Figure 3. The proposed system components

Figure 4. The implemented electronic circuit

Figure 5. The proposed system placement.

Results:

After testing the implemented system using the oscilloscope, the electrical pulses that should reached to the patient shows good values represented by 90V maximum voltage, 62 Hz , 600ms pulse width, and the will be depended on the tissue impedance of the user. These values are accepted values as they are within the range that make the stimulation occurs according to [6].

The figures 6 and 7 show the output waveform, pulses of the designed stimulator.

The wave form shows a biphasic type wave form, each pulse part is approximately the same in duration and magnitude to the other opposite polarity part, this will produce no or very small net charge in the body, which is considered more comfortable for stimulation when using surface electrode.

In the other hand, the train of pulses produced by the stimulator shows very accurate pulses produced with time regarding amplitude, frequency and duration. This will lead to active, accurate and constant with time stimulation.
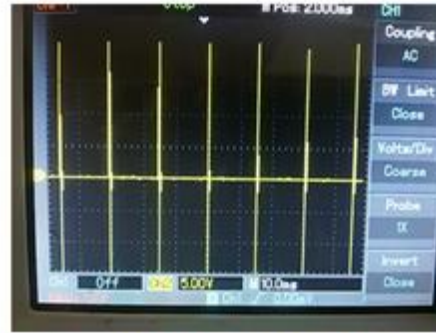
Figure 5. Output waveform of the stimulator.   Figure 6. Output pulses of the stimulator.

Conclusions

This research presented accurate foot drop prosthesis device, in which the output pulses are biphasic type leads to comfortable and accurate stimulation of the group of muscles responsible of lift the foot of the ground for foot drop patients. The simple and low cost components of the proposed system shows results suitable for daily uses by those patients easily, by fitted the electrodes externally on the targeted group of muscle, without the need for implanted electrodes. This user friendly design needs only to regulate the output voltage for one time only at the first time to use it, and then the same setting will be used for longtime, so it will decrease the time needed for training to the minimum limits.

References

[1]WeberDJ, et al."Functional electrical stimulation using microstimulators to correct foot drop: a case study",Can. J. Physiol. Pharmacol. Vol.82: 784–792, 2004.

[2]Michelle H Cameron. "The WalkAide® Functional Electrical Stimulation System – A Novel TherapeuticApproach For Foot Drop in Central Nervous System Disorders".European Neurological Review, 5(2):18–20 ,2010.

[3] William Horsley, "Orthotic functional electricalstimulation for drop footof neurological origin", NETAG, 2012.

[4] Richard B. Stein, et al. "A Multicenter Trial of a FootdropStimulator Controlled by a Tilt Sensor", Neurorehabilitation and Neural Repair, 20:371–379, 2006.

[5]MetinAkay, "The Wiley Encyclopedia of Biomedical Engineering",John Wiley & Sons, 2006.

[6]David Prutchi, Michael Norris, "Design and development of medical electronic instrumentation", John Wiley & Sons, 2005.

[7] Amanda E Chisholm, "Dropped Foot Impairment Post Stroke: Gait Deviations and the ImmediateEffects of Ankle-Foot Orthotics and Functional Electrical Stimulation",A thesis submitted in conformity with the requirementsfor the degree of Doctor of PhilosophyGraduate Department of Rehabilitation ScienceUniversity of Toronto© Copyright by Amanda E Chisholm, 2012.

[8] L.Vodovnik, S.Grobelnik," Multichannel functional electrical stimulation-facts and expectations", Prosthetics and Orthotics International, 1,43-46, 1977.

[9] Yoichi Shimada, et al, "Clinical Application of Acceleration Sensor to Detect the Swing Phase of Stroke Gait in Functional Electrical Stimulation", Tohoku J. Exp. Med., 207:197-202, 2005.

[10] James Moore, George Zouridakis, "Biomedical technology and devices handbook", CRC Press, 2004.

[11] John G. Webster, "Medical Instrumentation: Application and Design", John Wiley & Sons, 2010.

[12] Doug Lowe, Dickon Ross, "Electronics All-in-One For Dummies",John Wiley & Sons, 2014.

[13] Mike Tooley," Electronic circuits: fundamentals and applications", Routledge, 2015.

Analysis of Magneto Hydrodynamic of Second Order Fluid Flow in a Micro-Channel and heat Transfer between Two Parallel Plates

Wala'aAbdulMageed Mahdi

Abstract

In present study, analysis of magnetic field was studied in the state of non Newtonian fluid of second order flows and heat transfer in micro channel between two parallel plates, introduced. The equations are used to describe the flow are the motion and the energy equations. It found that these equations are controlled by many dimensionless numbers such as Reynolds number (Re), magnetic field parameter (M), physical quantity at wall (W), Knudsen number (Kn), Peclet number (Pe), Brinkman number (Br) and the material of fluid (α, β). The homotopy analysis method (HAM) is used to obtain the analytic solution for the velocity and heat transfer, the effect of each dimensionless parameters upon the velocity and heat distribution is analyzed and shown graphically by using MATLAB package.

Key words; Second order fluid, The velocity profile, The heat transfer.

تحليل المغناطيسية هيدروديناميكية لتدفق السائل
من الدرجة الثانية في قتاة الصغرى، ونقل الحرارة بين اثنين من لوحات الموازية

ولاء عبد المجيد مهدي

المستخلص

في هذا البحث دراسة الحقل المغناطيسي لجريان مائع لا نيوتيني من الرتبة الثانية وانتقال الحرارة في الانابيب الدقيقة بين صفيحتين متوازيتين ٫المعادلات التي استخدمت لوصف حركة المائع هي معادلات الحركة ومعادلة الطاقة وقدحلت تحليلياً باستخدام طريقة الهوموتوبي حيث وجد ان هذه المعادلات تحكمها اعداد لابعدية مثل عدد رينولدز،بلكت،هارتمان وثوابت اخرى تخص المائع. وقمنا بدراسة تأثير تلك الاعداد اللابعدية المذكورة.وقدتمت هذه الدراسة باستخدام البرنامج الجاهز الماتلاب.

الكلمات المفتاحية:سائل الدرجة الثانية ٫ توصيف السرعة ٫ نقل الحرارة

Introduction

Magneto-fluid dynamics (MHD) is that branch of applied mathematics, which deals with the flow of electrically conducting fluids in electric and magnetic fields. It unified in a common framework the electromagnetic and fluid-dynamic theories to yield a description of the concurrent effects of the magnetic field on the flow and the flow on the magnetic field.

In view of the abundant applications of non-Newtonian fluids in industry and technology, the interest in the study of such fluids has been increased during the last few years. Mathematicians and computer scientist have been involved in carrying out flow analyses of the non-Newtonian fluids in various aspects. Several constitutive expressions for these fluids have been suggested. These equations differ between the shear stress and rate of strain in view of the different characteristics of the non-Newtonian fluids. As a consequence of these constitutive equations, the resulting equations for non-Newtonian fluids in general are more complicated and of high order in comparison to the Navier- Stokes equations.

Considerable efforts have been devoted to studying the non-Newtonian fluids through analytic and numerical treatments. Some progress on the topic can be mentioned: in the studies [2, 11, 14-16]. In all of these studies, constant viscosity fluids (Newtonian fluids) are used.

A systematic research on micro devices started in the late 1980's.Micro ducts, micro nozzles, micro pumps, micro turbines and microvalves are the examples of the devices involving liquid and gas flows.

Modeling mass, momentum and energy transport may be necessary. Slip, rarefaction, compressibility, intermolecular forces andother unconventional effects. The Knudsen number (Kn) can classify thegas flow in micro channel into four flow regimes: continuum flow (Kn<0.001), slip flow (0.001 <Kn< 0.1), transition flow (0.1 <Kn< 10) and free molecular flow (Kn> 10) [5]. Since

Navier–Stokes (N–S) equations are not valid for Kn beyond 0.1, the lattice Boltzmann method (LBM) was developed as an alternative numerical scheme [23] and [19].However, for flows in continuum and slip regimes, Eckert and Drake [6] have indicated that there is strong evidence to use the N–S equations modified by boundary conditions. Tsien [20] originally designated theregime next to continuum flow as the "slip flow", following Maxwell and Smoluchowski in assuming that the first failure of continuum theory would occur at gas–solid interfaces, where the empirical conditions of continuity of tangential velocity and temperature should give way to the slip and temperature-jump boundary conditions. Studies of the continuum theory warn that in principle the N–S-plus-slip theory lacks internal consistency, but the try-it-and-see approach has yielded a substantial body of practically satisfactory results[19]and Liu [12] .

The Homotopy Analysis Method (HAM) is a powerful technique for solving linear and nonlinear partial differential equation ,for example the equation that appears in our problem . In most cases of nonlinear problems can be described by a set of governing linear equations with its initial / boundary conditions.[12].

The main paper that upon, is the work of Marwan, Ahmed. [17] ,they are studied of MHD on flow of Newtonian fluid and heat transfer between two plates .The governing non- linear problems have been solved analytically by using (HAM).

In this study HAM is employed to find the velocity, heat transfer of non- Newtonian fluid of second order by assumption:

1. Steady flow of incompressible fluid.
2. Two -dimensional and laminar fluid flow.
3. Constant fluid properties i,e C_p, k, μall remain constants.
4. Only conductive and convective energies in the flow are considered.

5. Heat generation on account of fluid friction (*known as viscous work*) being small (as the flow velocities are moderate). Finally, the results and discussions are given the effects of the various parameters of interest for the velocity and heat transfer.

2- Governing Equations:

Let (x, y, t) denote the Cartesian coordinates, $V=(u, v)$ is the velocity vector in these directions, and t is the time. As depicted in Fig 1, the inlet velocity and temperature are assumed to be uniform, the distance between the two parallel plates is 2d. The governing equations based on the Navier-stokes Equations with slip-flow boundary conditions. The process is assumed tobe two-dimensional steady (all derivatives w.r.t time are zero) laminar flow and the non-Newtonian fluid of second order. The body forces and the effect of compressibility are neglected and MHD on flow and heat transfer in micro-channels between two parallel plates.
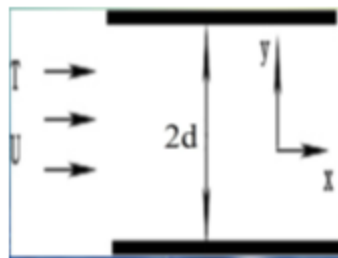

Figure 1. Microchannel between two parallel plates

The Caushy stress tensor in such a fluid is related to the motion equations in the following manner [7].

$$T=-PI+\mu A_1 + \alpha_1 A_2 + \alpha_2 A_1{}^2$$

$$\tag{1}$$

where $A_1 = \nabla V + (\nabla V)^T$

$$A_2 = \frac{dA_1}{dt} + A_1(\nabla V) + (\nabla V)^T A_1 \tag{2}$$

$$\mu \geq 0, \ \alpha_1 \geq 0, \alpha_2 \geq 0 \tag{3}$$

In this equation, P is the pressure, V is the velocity vector, ∇ is the gradient oparoter, $\alpha_i(i=1,2)$ are the material moduli of fluid ,d/dt is the material derivative, and $A_i(i=1,2)$ are the two first Rivilin Eriksen tensor .

Note that for $\alpha_1, \alpha_2 = 0$ equation (1) along with (2) descries of Newtonian fluid [17].

In addition to (1) the basic equations of the problem are in the following:

28

$$\nabla V = 0 \quad (4)$$

$$(\nabla V) = \nabla T + (J \times B) \tag{5}$$

$$\rho Cp(V\nabla T) = K\Delta T \tag{6}$$

Equations (4),(5) and (6) are the continuity, momentum ,and energy equations respectively .Where ρ is the density and $(J\times B)$is Lorenz force vector .The fluid is assumed to be steady and laminar .substituting the stress tensor T from (1) into (5)yields:

$$\rho(V\nabla V) = -\nabla P + \mu(\nabla^2 V)\sigma u B^2 \tag{7}$$

The velocity components corresponding to X ,Y direction respectively denoted by u ,v, following [15] , compatible with the continuity of the form :

$$u = \frac{Ux}{H} f'(\eta), v = -Uf(\eta) \tag{8}$$

where$\eta = y/H$ and the prime denoted the differential with respect to η

The boundary conditions for the velocity field are :

$$f''(0) - Knf'(0) = 0 \quad , \quad f''(0) = -1 \quad , f''(10 = 0 \tag{9}$$

It follows from (7) and equation of motion that :

$$\frac{\partial P}{\partial x} = \frac{Ux}{H^2}[Re(ff'' - f'^2) + f''' - Mf' + \alpha(-ff'''' + 2f'f''' + 3f''^2) + \beta(2f''^2)]$$

$$\tag{10}$$

$$\frac{\partial P}{\partial y} = -Reff' - \frac{\mu U}{H}[f'' + \alpha\left(ff''' + 6f'f'' + \frac{8x^2}{H^2}f''f'''\right) + \beta\left(8f'f'' + \frac{2x^2}{H^2}f''f'''\right)]$$

(11)

Where the cross –flow Reynolds number ,Re, M is the Hartmann number(MHD) number, and α,β are the dimensionless numbers ,are defined through respectively.

$$Re = \frac{\rho UH}{\mu} \quad , \quad M = \frac{\sigma u B^2}{\mu} \quad , \quad \alpha = \frac{U\alpha_1}{\mu H}, \quad \beta = \frac{U\alpha_2}{\mu H}$$

(12)

The derivative of equation(10) w.r.t y gives

$$\frac{\partial}{\partial y}\left(\frac{\partial P}{\partial x}\right) = 0 \tag{13}$$

It can be concluded from the last equation that the function $\frac{\partial P}{\partial x}$ isindependent of variable y, which means we can assume:

$$\frac{\partial P}{\partial x} = C_x \quad (14)$$

Where C_x is a constant

By using equation (14) into (10)

$$\frac{H^3}{vUx} C_x = [Re(ff'' - f'^2) + f''' - Mf' + \alpha(-ff'''' + 2f'f''' + 3f''^2) + \beta(2f''^2)]$$

$$(15)$$

It is apparent that the quantity in parentheses in (15) must be independent of η. Hence, the following equation for f is:

$$[Re(ff'' - f'^2) + f''' + W - Mf' + \alpha(-ff'''' + 2f'f''' + 3f''^2) + \beta(2f''^2)] = 0$$

$$(16)$$

Where $W = \frac{H^3}{vUx} C_x$ is the physical quantity atwall

Note that the equations (11),(12),(13),(15) and (16) becomes in Newtonian flow [17] where we put α and $\beta = 0$.

Equations for Temperature3- Governing

In this section ,temperature field as below

$$\theta(\eta) = \frac{H}{x^2} \frac{(T_1 - T_0)}{(T - T_\circ)} \quad (17)$$

where T_0, T_1 are the temperatures and with constant value. Substituting (8) and (17) into (6) lead to the following equation:

$$\theta'' + Brf''^2 - 2Pef'\theta + Pef\theta' = 0$$

$$(18)$$

Where $Br = \frac{1}{\lambda} \frac{\mu U^2}{T_1 - T_0}$ Pe $= \rho UHcp/k$ is the Peclet number .Equation (18) is solved subject to the boundary conditions

$$\theta(0) - Kn\theta(0) = 0, \quad \theta''(1) = 1$$

$$(19)$$

4- Solution Using Homotopy Analysis Method

In this section HAM is applied to solve (16) subject to the boundary conditions (9) .The initial guesses and linear operators are chosen in the following :

$$f_0(\eta) = \frac{1}{6}\eta^3 - \frac{1}{2}\eta^2 - Kn\eta \quad (20)$$

As the initial guess approximation for $f(\eta)$ is

$$L_1(f) = f''''\quad(21)$$

As the auxiliary linear operator has the property:

$$L(c_1 + c_2\eta + c_3\eta^2 + c_4\eta^3) = 0\quad(22)$$

And $c_i(i = 1 - 4)$ are constant. Let $p \in [0,1]$ denotes the embedding parameter and h indicates non zero auxiliary parameters .Then the following equation are constructed:

$$(1 - p)L_1(f(\eta; p) - f_0(\eta)] = ph_1 N_1[f(\eta; p)]\quad(23)$$

$$f'(0;p) - Kn\, f''(0;p) = 0 \ , f(0;p) = 0, f''(0;p) = 0, f''(1;p) = 1$$

$$(24)$$

$$N_1[f(\eta; p)] = f'''(\eta; p) + Re(f'(\eta; p)f(\eta; p) - f'(\eta; p)f'(\eta; p)) - Mf'(\eta; p) + W +$$
$$\alpha(-f(\eta; p)f''''(\eta; p) + 2f'(\eta; p)f'''(\eta; p) + 3f''(\eta; p)f''(\eta; p)) + \beta 2(f''(\eta; p)f''(\eta; p))$$
$$=0$$

$$(25)$$

for p=0 and p=1:

$$f(\eta; p) = f_0(\eta) \ , \quad f(\eta; 1) = f(\eta) \quad (26)$$

When p increases from 0 to 1 then $f(\eta; p)$ vary form $f_0(\eta)$ to $f(\eta)$.By using Taylor's theorem and using (23):

$$f(\eta; p) = f_0(\eta) + \sum_{m=1}^{\infty} f_m(\eta)p^m,$$

$$f_m(\eta) = \frac{1}{m!}\frac{\partial^m(f(\eta;p))}{\partial p^m}\quad(27)$$

$$f(\eta) = f_0(\eta) + \sum_{m-1}^{\infty} f_m(\eta) \quad (28)$$

mth $-$ order deformation equations are: The

$$L[(f_m(\eta) - X_m f_{m-1}(\eta)] = hR^f{}_m(\eta),\quad\quad\quad(29)$$

The boundary conditions are:

$$f'_m(0) - Kn f''_m(0) = f_m(0) = f''_m(1) = 0, f''_m(0) = -1 \tag{30}$$

Where $R^f_m(\eta) = f''' + \text{Re}$

$$\sum_{i=0}^{m-1}(f_{m-1}f''_i - f'_{m-1}f'_i) + W(1 - X_m) - M f'_{m-1} + \alpha(\sum_{i=0}^{m-1}(-f_{m-1}f''''_i + 2f'_{m-1}f'''_i + 3f''_{m-1}f''_i)) + \beta\sum_{i=0}^{m-1} 2f''_{m-1}f''_i$$

(31)

$$X_m = \begin{cases} 0 & m \le 1 \\ 1 & m > 1 \end{cases} \tag{32}$$

To find the solution of m th -order deformation, we shall use the symbolic software MATLAB up to first few order of approximation. We found the solution up to 2 the order approximation and they are:

$f_1 =$- (Re*h* η ^8)/20160 + ((Re*h)/2520 + (α*h)/2520)* η ^7 + ((α*h)/180 - (Re*h)/720 - (M*h)/720 + (β*h)/180)* η ^6 + ((M*h)/120 - (α*h)/20 - (β*h)/30 - (Re*h*kn)/120 - (α*h*kn)/60)* η ^5 + (- (Re*h*kn^2)/24 + (M*h*kn)/24 + h/24 + (W*h)/24 + (α*h)/8 + (β*h)/12)* η ^4 + η ^3/6 - η ^2/2 - kn* η

$$\begin{aligned}
f_2 = {}& \eta^7 * ((\alpha*h)/5040 - (\text{Re}*h)/2520 - (M*h^2)/2520 - (\text{Re}*h^2)/5040 + (\alpha \\
&*h^2)/336 + (\beta*h^2)/315 + (17*\alpha^2*h^2)/1680 + (\beta^2*h^2)/126 \\
&- (M^2*h^2*kn)/5040 + (3*\alpha^2*h^2*kn)/280 + (\alpha*h*kn)/1260 \\
&+ (\text{Re}^2*h^2*kn^3)/5040 + (\alpha^2*h^2*kn^2)/420 - (M*W \\
&*h^2)/5040 - (M*\alpha*h^2)/840 - (M*\beta*h^2)/840 + (11*W*\alpha \\
&*h^2)/5040 + (W*\beta*h^2)/420 - (\text{Re}*h^2*kn)/5040 + (47*\alpha*\beta \\
&*h^2)/2520 - (\text{Re}*W*h^2*kn)/5040 + (M*\alpha*h^2*kn)/2520 + (M*\beta \\
&*h^2*kn)/420 - (\text{Re}*\alpha*h^2*kn)/1680 + (\text{Re}*\beta*h^2*kn)/2520 + (11 \\
&*\alpha*\beta*h^2*kn)/1260 - (\text{Re}*\alpha*h^2*kn^2)/1008 - (\text{Re}*\beta*h^2 \\
&*kn^2)/420) - \eta^{15}*((\text{Re}*\alpha^2*h^3)/70761600 - (M*\text{Re}^2 \\
&*h^3)/412776000 - (\text{Re}^3*h^3)/707616000 + (31*\text{Re}^2*\alpha \\
&*h^3)/1651104000 + (19*\text{Re}^2*\beta*h^3)/1238328000 + (\text{Re}^3*h^3 \\
&*kn)/990662400 - \cdots \ldots\ldots\ldots\ldots\ldots..
\end{aligned}$$

5- Converge of solution (4)

We notice that the explicit analytical expression in eq.(29) contain the auxiliary parameter h_1.As pointed out by Liao [15] ,the convergence region and the rate of approximations given by the HAM are strongly depending on h_1. By means of so-called h-curve for the velocity profile figure

(2). The range of admissible value of h_1 for the velocity profile   is $-0.8 \leq h_1 \leq 0.8$.   For the velocity distribution, tables (1) and (2) illustrate the values of the first
and second derivatives for different order of the approximations . It is noted that
the best value for h is-0.2.

values of h_1	$\dfrac{f'}{f_0 + f_1 + f_2}$
-0.8	-1.9831
-0.6	-1.4873
-0.4	-0.9914
-0.2	-0.49581
0.2	0.4958
0.4	0.9916
0.6	1.4873
0.8	1.9831

Table (1)the values of the convergence parameter h using the first derivative.

Values of h_1	$\dfrac{f''}{f_0 + f_1 + f_2}$
-0.8	-14.2203
-0.6	-8.9843
-0.4	-5.1173
-0.2	-2.2467
0.2	1.9953
0.4	4.1115
0.6	6.7215
0.8	10.1972

Table (2)the values of the convergence parameter h using the second derivative.

6- - Solution Using Homotopy Analysis Method

   In this section HAM is applied to solve (18) subject to the boundary conditions (19). The initial guesses and linear operators are chosen in the following :

$$\theta_\circ(\eta) = Kn - \frac{1}{2}\eta^2 \quad (33)$$

As the initial guess approximation for $\theta(\eta)$ is

$$L_2(\theta) = \theta'' \quad (34)$$

As the auxiliary linear operator has the property:

$$L(c_1 + c_2\eta) = 0 \quad (35)$$

And $c_i (i = 1 - 2)$ are constant. Let $p \in [0,1]$ denotes the embedding parameter and h indicates non zero auxiliary parameters .Then the following equation are constructed:

$$Zeroth - order\ deformation\ equations$$

$$(1 - p)L_2(\theta(\eta; p) - \theta_0(\eta)] = ph_2N_2[\theta(\eta; p)] \quad (36)$$

$$\theta(0;p)\text{-}Kn\ \theta'(1;p) = 0, \qquad \theta(1;p) = 1$$

$$\tag{37}$$

$$N_2[\theta(\eta; p)] = \theta''(\eta; p) - Brf''^2(\eta; p) + Pe(f(\eta; p)\theta'(\eta; p) - 2Pe(f'\eta; p)\theta(\eta; p)) = 0$$

$$\tag{38}$$

for p=0 and p=1:

$$\theta(\eta; 0) = \theta_0(\eta) \quad , \qquad \theta(\eta;1) = \theta(\eta) \qquad (39)$$

When p increases from 0 to 1 then $\theta(\eta; p)$ vary form $\theta_0(\eta)$ to $\theta(\eta)$.By using Taylor's theorem and using (36):

$$\theta(\eta; p) = \theta_0(\eta) + \sum_{m-1}^{\infty} \theta_m(\eta)p^m, \quad \theta_m(\eta) = \frac{1}{m-2!} \frac{\partial^m(\theta(\eta;p))}{\partial p^{m-2}}$$

$$\tag{40}$$

$$\theta(\eta) = \theta_0(\eta) + \sum_{m-1}^{\infty} \theta_m(\eta) \quad (41)$$

The mth $-$ order deformation equations

$$L[(\theta_m(\eta) - X_m\theta_{m-1}(\eta)] = hR^\theta{}_{m-1}(\eta), \qquad (42)$$

The boundary conditions are:

$$\theta_m(0) - Kn\theta'_m(0) = \theta_m(1) = 0 \quad (43)$$

Where $R^\theta{}_{m-1}(\eta) = \theta''_{m-1} + Br\sum_{i=0}^{m-1}(f'''_i f'_{m-1-i}) + Pe$

$\sum_{i=0}^{m-1}(f_i\theta'_{m-1-i}) - 2Pe\sum_{i=0}^{m-1}(f''_i\theta_{m-1-i})$

(44)

$$X_m = \begin{cases} 0 & m \leq 1 \\ 1 & m > 1 \end{cases} \quad (45)$$

To find the solution of m th -order deformation, we shall use the symbolic software MATLAB up to first few order of approximation . we found the solution up to 2nd. order approximation and they are:

θ_1= Kn - η - η ^3*((Br*h)/3 - (Pe*h*kn)/6) - η ^4*((Pe*h)/8 - (Br*h)/12 + (Pe*h*Kn)/12) + η ^2*(Pe*h*kn^2 - h/2 + (Br*h)/2) - η ^2/2 + (Pe*h* η ^5)/60 + (Pe*h* η ^6)/90

$\theta_2 = kn - \eta + \eta^2 * (Br * h - h/2 + (Br * h^2)/2 - h^2/2 + Pe * h^2 * kn^2 + 2 * Pe * h * kn^2) - \eta^3 * ((Br * h)/3 - (Pe * h * kn)/6) + \eta^{10} * ((11 * Pe * Re * h^2)/604800 + (Pe * a * h^2)/37800) - \eta^4 * ((Pe * h)/8 - (Br * h)/12 + (Pe * h * kn)/12) + \eta^2 * (Pe * h * kn^2 - h/2 + (Br * h)/2) - \eta^3 * ((2 * Br * h)/3 + (Br * h^2)/3 - (Pe * h * kn)/3 - (Pe * h^2 * kn)/6) - \eta^4 * ((Pe * h)/4 - (Br * h)/6 + (Pe * h^2)/8 + (Pe * h * kn)/6 + (Br * W * h^2)/12 + (Br * a * h^2)/4 + (Br * \beta * h^2)/6 + (Pe * h^2 * kn)/12 + (Br * M * h^2 * kn)/12 - (Br * Re * h^2 * kn^2)/12) - \eta^9 * ((Pe^2 * h^2)/5184 + (Br * Re * h^2)/12960 + (M * Pe * h^2)/10368 + (Pe * Re * h^2)/40320 - (.......$

-

7- Converge of solution (6)

We notice that the explicit analytical expression in eq.(24) contain the auxiliary parameter h_2. As pointed out by Liao [15] ,the convergence region and the rate of approximations given by the HAM are strongly depending on h_2.. By means of so-called h-curve for the heat transfer profile figure (4). The range of admissible value of h_2 for the heat rang   is $-0.8 \leq h_2 \leq 0.8$. For the heat distribution, table (3)   illustrate the values of the firstderivatives for different order of the approximations . It is noted thatthe best value for h is-0.2.

Value of h_2	$\dfrac{\theta'}{\theta_0 + \theta_1 + \theta_2}$
-0.8	-4.3513
-0.6	-4.6346
-0.4	-5.0038
-0.2	-5.4590
0.2	-6.6270
0.4	-7.3398
0.6	-8.1386
0.8	-9.0233

8-Result and discussions:

8-1 The velocity profile :

In this section the effect of Reynolds number "Re" , the MHD parameter "M" , the Knudsen "kn" ,physical quantity at wall "W" ,and the materials of fluid "α,β"were examined

- Figure(4) shows the effect of dimensionless Reynolds number "Re" , in which the values of parameter "M" , the Knudsen "kn" ,physical quantity at wall "W" ,and the materials of fluid "α,β" are (1,0.1,1,1,2) respectively , Reynolds number "Re" is kept by values (7,8,9) the following result is obtained :when Reynolds number "Re" is increases then the velocity profile is increases too.

- In effect of parameter "M" ,the values ofdimensionless Reynolds number "Re" , the Knudsen "kn" ,physical quantity at wall " W" ,and the materials of fluid "α,β" (7,0.1,1,1,2)respectively ,and (1,5,10) were the values of MHD parameter "M" . As MHD parameter "M" increases a decrement in the velocity profile see figure(5) .
- To study the effect of dimensionless Knudsen "kn" the values of

of Reynolds number "Re" , the MHD parameter "M" , ,physical quantity at wall "W",the materials of fluid "α,β" were fixed (7,1,1,1,2) respectively , and dimensionless Knudsen "kn" is taken the values (0,0.1) the following results are obtained: The values of velocity increases when Knudsen "kn" increases see figure

(7)

- Figure(8,9) illustrates the effect of dimensionless parameter ,β,α on the velocity profiles for fixed Re=7,M=1,kn=0.1,W=1 ,β=2,6,8 and α= 1,5 ,10 It is obvious from this figure that the effects of α ,β is very strong   on the velocity profile where it increases,because the value of the velocity became very small   and if α =0 and β = 0,then the velocity profile would be verified by flow of Newtonian fluid cases[17].

- Figure(6) depicts the velocity for Re=7,M=1 kn=0.1, $\alpha = 1, \beta = 2$ It is obvious for this figure that the velocity decreases if the value of W is large.

8-2 The heat distribution :

- Figure(14) depicts the profiles of temperature in viscoelastic fluid .when Re=7 ,M=1, $\alpha = 1$, β =2,that the effect of Peclet number on temperature   profile is shown .According to definition of Peclet number,   increasing of Peclet number leads to   increases   in the temperature distribution in micro channel.
- Figure(10,11) illustrates the effect of dimensionless parameter $, \beta, \alpha$ on the heat transfer   for fixed Re=7,M=1,kn=0.1,W=1 ,Pe=1 and Br=1 It obvious from this figure that α, β is heavily affect   on the heat transfer where it increases, and if α =0 and $\beta = 0$,then the flow fluid becomes of Newtonian [17].

- The heat transfer is fixed , when the Knudsen "kn" is increasing see figure(12).

- Figure (13) illustrates the effect of physical quantity at wall "W" for fixed Re=7,M=1,kn=0.1, $\alpha = 1 , \beta = 2$,Pe=1 and Br=1 It obvious that the heat is increasing when W increased .

- In effect of parameter "Br" ,we kept the values of dimensionless Reynolds   number "Re" , the Knudsen "kn" ,physical quantity at wall "W" , Pe=1 and the materials of fluid "α,β" by (7,0.1,1,,11,2)respectively ,. As parameter "Br" increases there is decreasing in the heat transfer see figure 15.

9- Conclusions:

The flow of second order fluid in a micro channel is studied by Homotopy Analysis method   in this paper ,and the approximate   analytic solutions are obtained .The major conclusions in the research are :

1- When the fluid flow .The Reynolds number Re, the magneto number M , the Kundsen number Kn, the physical quantity at wall W, and the non Newtonian parameters α,β affect the velocity profile and heat distribution .
2- The effect of non Newtonian parameters α,β   is   so effective that lead to decrease on the velocity .
3- In general Kundsen number Kn in significant effect in which the resultant increment   in velocity and heat transfer is very low .
4- When taking a gradually increased values for Pe ,this lead to increases in temperature ,according to Pe definition this may carve an equal distribution of heat at both sides of the channel .
5- Increasing Br leads to decreases in heat transfer .
6- At certain high temperature when α is taken large ,heat transfer starts decreases while when a high value of β is taken , will be heat transfer start to increase .
7- When taking   increased values for   physical quantity at wall W ,this lead to decreases in the velocity and increases in the heat transfer .

References :

[1] Anderas A. (2001), "Principle of fluid mechanics", Printice-Hill, Inc.

[2] Allan F.M., M.I. Syam (2005), "On the analytic solution of nonhomogeneous Blasius problem" J. Comput. Appl. Math. 182 (2) , pp. 362–371.

[3] Abbasband S. (2006) "The application of the homotopy analysis method to nonlinear equations arising in heat transfer" Phys. Lett. A, 360 (1) , pp. 109–113.

[4] Abbasband S. (2007) "The application of homotopy analysis method to solve a generalized Hirota–Satsuma coupled KdV equation" Phys. Lett. A, 361 (6) ,pp. 478–483.

[5] Beskok A. , G.E. Karniadakis (1994) " simulation of heat and momentum transfer in complex micro-geometries", AIAA J. Thermophys. Heat Transfer, 8 (4) , pp. 355–370.

[6] Eckert E.G.R., R.M. Drake Jr. (1972) " Analysis of heat and mass transfer" McGraw-Hill, New York ,pp. 467–486.

[7] Fosdick R.L., Rajagopal ,K. R. (1980), "Thermodynamic and stability of fluids ". Proc.R. Soc. London. A339-351.

[8]Gramer K. R. and Pai-Shih-1(1973), "Magnetofluiddynamics for engineers and applied physics", McGraw-Hill Book Company, New York.

[9] Huba J. D. (1994), "NRL Plasma formulary, Naval research laboratory.

[10] Hayat T., M. Sajid (2007)"On analytic solution for thin film flow of a fourth grade fluid down a vertical cylinder" Phys. Lett. A, 361 (4) ,pp. 316–322.

[11] Kenyon E. (1980), "Fluid mechanics", John Wiley and sons.

[12] Liu J.Q., Y.C. Tai , C.M. Ho ,(1995) "MEMS for pressure distribution studies of gaseous flows in microchannels, in: Proceedings of the micro electro mechanical systems", IEEE, pp. 209–215.

[13] Liao S.J., (1992)"Proposed Homotopy Analysis Techniques for the Solution of Nonlinear Problems", PhD Thesis, Shanghai Jiao Tong University, Shanghai,.

[14] Liao S.J. An explicit, (1999) " totally analytic approximation of Belasis viscous flow problems" Int. J. Non Linear Mech. 34 (4) , pp. 759–778.

[15] Liao S.J. (2004)"On the homotopy analysis method for nonlinear Problems Appl".Math.Computer., 147 (2), pp. 499–513.

[16] Liao S.J. (2005) "A new branch of solutions of boundary-layer flows over an impermeable trenched plate" Int. J. Heat Mass Transfer, 48 (12) , pp. 2529–2539.

[17] Marwan A. ul-SatarandAhmedM.Hadi (2013) "The influence of MDH of Newtonian fluid and heat transfer between tow plates by using HAM". University of Baghdad .

[18] Sherman F.S. (1969)" The transition from continuum to molecular flow" Annu. Rev. Fluid mech., 1 ,pp. 317–340.

[19] Tang G.H., W.Q. Tao, Y.L. He, (2005), " Lattice Boltzmann method for gaseous micro flows using kinetic theory boundary conditions" phys. Fluids, 17 (5) ,p. 058101.

[20] Tsien H.S. TsienSuperaerodynamics (1946), " mechanics of rarefied gases", J. Aerosp. Sci., 13 (12) , pp. 653–664.

[21] White F. B. (1994), "Fluid mechanics", McGraw-Hill, Inc., New York.

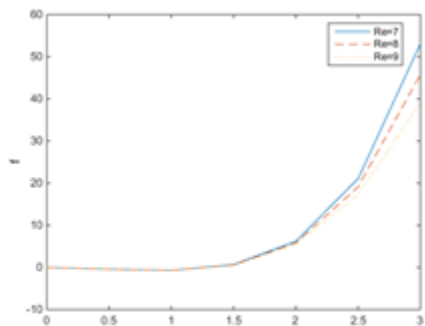[22] Wylie E. B. and Streeter V. L. (1983), "Fluid mechanics", McGraw-Hill Ryeson Limited.

[23] Zhang Y., R. Qin, D.R. Emerson (2005) "lattice boltzmann simulation of rarefied gas flows in micro channels", Phys. Rev. E, 71 (4), pp. 047702.
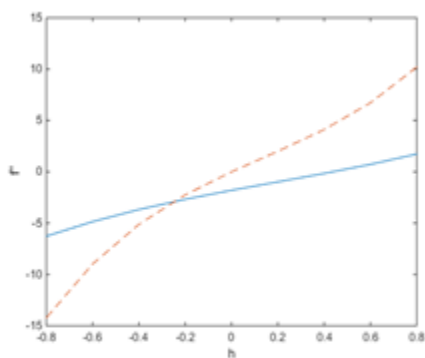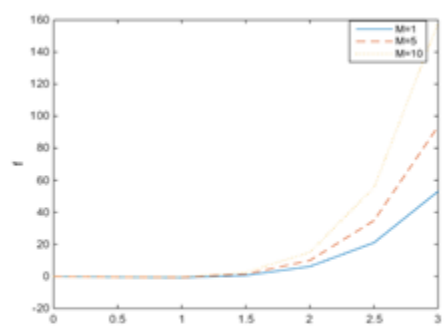
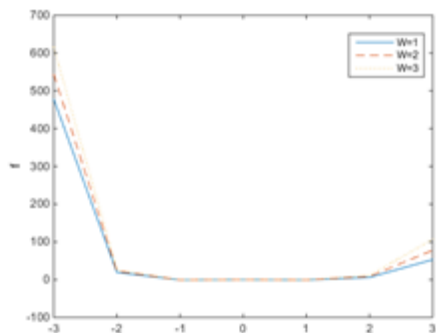Fig.(2) the h curve for the velocity profile
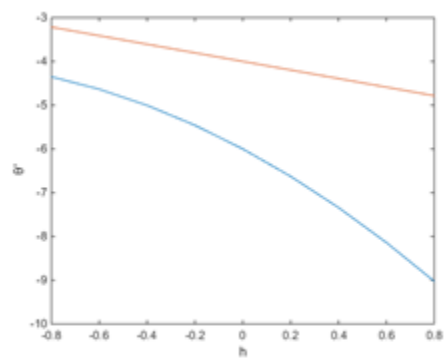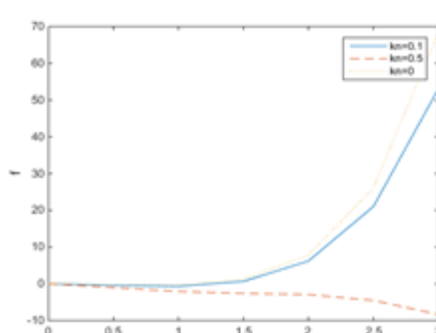
Fig.(3) the h curve for the heat transfer
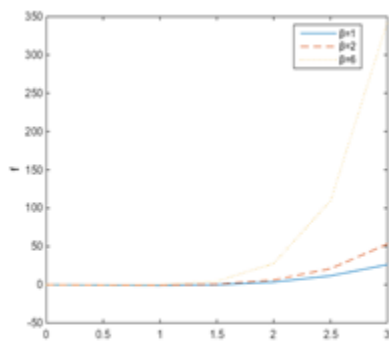
Fig(4) the effects of Re number on the velocity
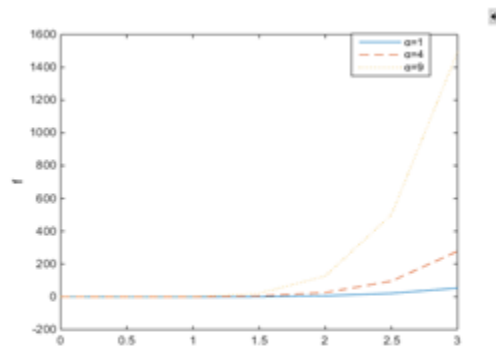
Fig(5) the effects of MDH number M on the velocity

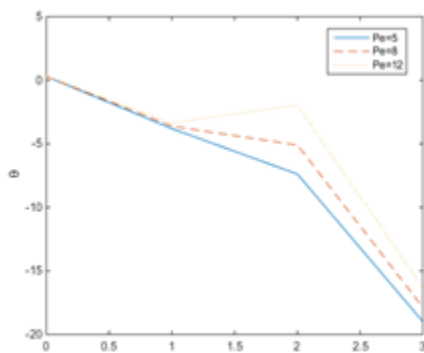Fig(6) the effects of W at the wall on the velocity

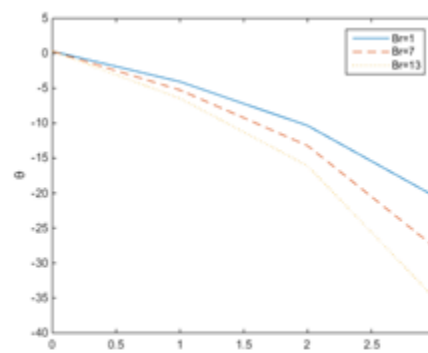Fig(7) the effects of Kn number on the velocity
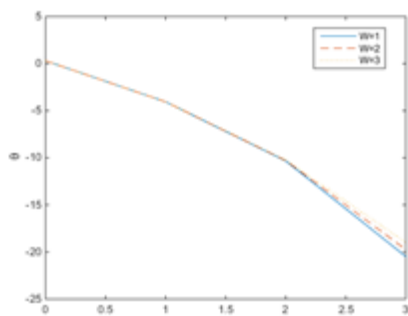
Fig(8) the effects of a parameter β on the velocity
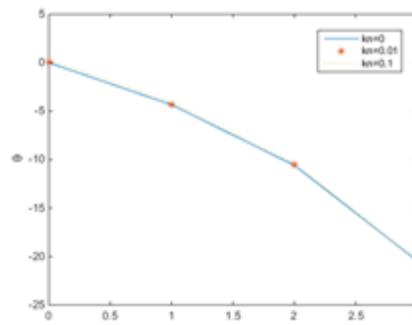

Fig(9) the effects of a parameter α on the velocity
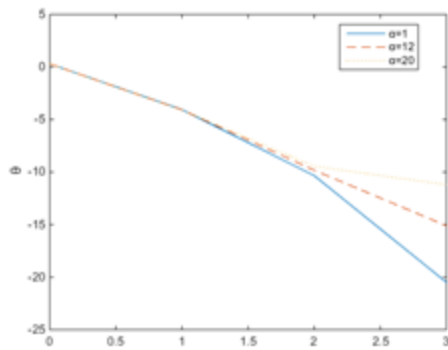

Fig(10) the effects ofPe number on the heat

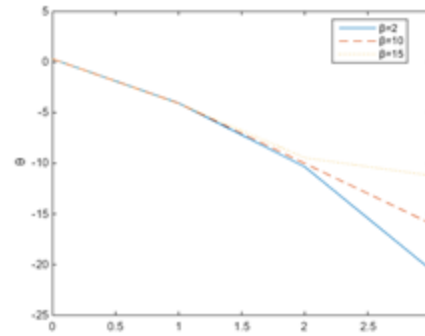Fig(11) the effects of Br number on the heat

Fig(12) the effects of W on the heat

Fig(13) the effects ofKn number on the heat

Fig(14) the effects of a parameter α on the heat   Fig(15) the effects of a parameter β on the heat

Notations:

There are many symbols are used in this paper :

∇: The gradient vector

V :The velocity vector of two dimensions

u: The velocity in X direction , v: the velocity in y direction

t:The time

T:TheCaushy stress tensor

A_1, A_2: The two first Rivilin -Erilksen tensor

α_1, α_2: The material moduli of fluid

J×B: Lorenz force vector , J×B:$=\sigma u B^2$

P: The pressure ,ρ: the density

K:The thermal conductivity

C_p: The specific heat

μ: The dynamicviscosity   , v: the kinematic viscosity

U: The uniform velocity ;   H: The height (boundary)

Re: Reynolds number , Re=$\dfrac{\rho UH}{\mu}$,   M: the magneto number ,M=$\dfrac{\sigma u B^2}{\mu}$

$\propto, \beta$: Non dimensionless parameters ,$\propto=\dfrac{U\alpha_1}{\mu H}$,   β=$\dfrac{U\alpha_2}{\mu H}$

W :The physical quantity at wall ,W=$\dfrac{H^3}{v U x} C_x$

T_0, T_1: The temperature

Pe: Peclet number , Pe=$\rho U H C_p / H$

Br:Brinkman number ,Br=$\frac{1}{\lambda} \frac{\mu U^2}{T_1 - T_0}$

Kn: Knudsen number ,Kn=$2 \frac{l}{y}$

Effects of L-methionine-DL-Sulphoximine(MSO) and 3-(3,4-dichlorophenyl)-N-N-dimethylurea(DCMU) on Physiological Activity of Cyanobacteria *Nostoc species* Isolated from Lichen *Peltigeracanina*

Jabbar F- Al-maadhidi
Department of Biology, Madenat Al-elem University College.
Baghdad, Iraq.
E-mail: dral_maadhidi@yahoo.com

Abstract
Lichen is a Symbiotic system consist of nitrogen fixing Cyanobacteria or and algae and fungus. Cyanobacteria can fix nitrogen in a peculiar differentiated cells called heterocyst under aerobic conditions, those heterocyst are the loci of nitrogenase activity. The organic nitrogen and carbohydrates produced by cyanobacteria utilized by fungi and the fungus supplying the cyanobacteria and algae by inorganic metals coming from dissolved rocks by acids produced by fungi. Culture of *Nostocspp* treated with MOS excreted, the newly fixed nitrogen in form of ammonia into liquid media, which is proportions with the concentration of the analog and detected after 6 h of treatment. Acetylene reduction technique (nitrogenase activity) was not affected by analog (MSO) treatment. The growth of Cyanobacteria *Nostocspp* was slightly inhibited starting after 6 h of treatment. The rates of carbon fixation were highly enhanced after treatment leading to increase the number of (PGBS) in the Cyanobacteria cells. The combination treatment of *Nostocspp* culture by MSO and DCMU showed the following: carbon and nitrogen fixation are dependent of each other, slight inhibitions in culture growth, 50% inhibition in ammonia release, complete inhibition of carbon fixation and disappeared of extra PGB. Light intensities and carbon fixation are dependent even in the presence of MSO. The cultivation of *Nostocspp* culture under $Ar/O_2/CO_2$ in presence of MSO gives reverse relationship between the cellular incorporated carbon and time. Electron micrograph showed an increase in PGBs of the lichen *P. conina* treated with MSO through the first hour of treatment and then disappeared after 24 h.

Key words: MSO, DCMU, Nitrogen fixation, Lichen.

تأثير كل من DCMU, MSO على الفعاليات الفسلجيه لخلايا السيانوبكتريا .Nostoc spp المعزولة من الاشن Peltigeraconina

جبار فرحان المعاضيدي

كلية مدينة العلم الجامعة / قسم علوم الحياة

الملخص

اظهرت المزارع الخلوية للنوع .Nostoc spp المعاملة بمادة MSO قدرتها على افراز الناتروجين ألمثبت حديثاً الى الوسط الزرعي السائل بعد ستة ساعات من المعامله على شكل امونيا وان الكمية المفروزة تناسب طردياً مع تركيز مادة MSO. لم تتاثر فعالية انزيم النتروجينيتز بمعاملة الـ MSO, في حين كان هناك تثبيط بسيط في النمو مما ادى الى زيادة في اعداد جسيمات PGBS في السايتوبلازم للخلايا. ان تداخل معاملة الخلايا للنوع .Nostoc spp بمادة MSO وبـ DCMU اوضحت الاتي : ان عملية تثبيت الكاربـــــون والنتروجين معتمدان بعضهما على البعض , تثبيط بسيط في نمو الخلايا, تثبيط 50% من امونيا المفروزة خارج الخلية , تثبيطكاملتثبيت الكاربون واختفاء جسيمات PGB الزائدة , شدة الاضاءة وتثبيت الكربون يعتمدان على بعضها حتى في حالة معاملة الخلايا بمادة MSO , ان تنمية المزارع الخلوية للنوع .Nostoc spp المعاملة بمادة MSO تحت خليط مـن $Ar/O_2/CO_2$ ادى الى علاقة عكسية بين الكاربون الخلوي التركيبي والزمن المعتمد في تنمية الخلايا , كما تبين دراســـة المجهر الالكتروني لعينات لآسنات من النوع .P. canina المعاملة بمادة MSO ازدياد عدد جسيمات PGBS خلال الساعة الاولى من المعاملة واختفائها كلياً بد 24 ساعة من المعامـــــلة .

Introduction

Lichen is a Symbiotic system consist of nitrogen fixing Cyanobacteria or and algae and fungus [1,2]. Cyanobacteria can fix nitrogen in a peculiar differentiated cells called heterocyst under aerobic conditions, those heterocyst are the loci of nitrogenase activity [3]. The organic nitrogen and carbohydratesproduced by cyanobacteria utilized by fungi, and the fungus supplying the cyanobacteria and algae by inorganic metals coming from dissolved rocks by acids produced by fungi [4]. In Legume nodules, the first product of N_2 fixation in bacteroids is NH_3. The NH_3 is then exported to the host plant cytosol where it is further metabolized to amino acids and amides [5]. Glutamine Synthase (GS) plays a key role in nitrogen metabolism, thus the fine regulation of this enzyme in *Prochloroccus*, which is especially important in the oligotrophic oceans where this marine *Cyanobacterium thrives* [6]. Metabolism of c14 glutamate showed that in white light glutamine was the main labeled product and in the dark label was principally in compounds closely associated with tri carboxylic acid cycle metabolism [7]. Also, glutamine synthase (GS) rapidly converts blood – borne ammonia into glutamine which in high concentration may cause mitochondrial dysfunction and osmotic brain edema [8], and it has been proposed that elevated glutamine levels during hyper ammonia lead to astrocyte swelling and cerebral edema using MSO as inhibitors for nitrogen metabolism [9].

The symbiotic relation in lichen components (algae, cyanobacteria and fungus) sharing the nitrogen and carbon fixed which affecting the physiological activity of all organisms in lichens. Nitrogen metabolism as a function of GS can inhibited by glutamine analog MSO, and carbon fixation (photo system II) can inhibited by DCMU [3,10-13].

In this study MSO and DCMU were used to explain the relationship between nitrogen fixation and carbon fixation in lichen (lichen system), the flow of fixed nitrogen, and the inhibition in growth of *Nostocspp.*isolated from lichens *peltigeraconina.*

Materials and methods

Organisms and culture conditions

The alga *Nostocspp* isolated from the lichen peltigeracanina at the Department of microbiology. Sciences University of Dundee, UK was grown in the N-free medium [14] under continuous culture conditions. The light intensity was 3000 lux and the temperature 26 ℃. Aliquots of alga were withdrawn regularly for experimental purposes, all experiments mentioned below were conducted at 3000 lux, 26 ℃ and with gentle shaking.

Effects of MSO and DCMU on some algal physiological processes

Effects of MSO on the relation between alga and fungus within symbiotic systems in lichens was studied in experiments carried out in conical flasks of 200ml capacity containing 50ml algal suspension (batch culture) treated with freshly prepared 0.5, 1.0, and 2 μm of MSO. Algal suspension without MSO served as control. Samples were regularly withdrawn during the period of the experiment (24 h) and assayed for (a) ammonia released to the medium (15), (b) rates of 14 CO_2 for 30 min being fixed intracellular and released to the medium (16),(c) algal growth chlorophyll a (17), and (d) nitrogenase activity (18). Algal samples were fixed at the beginning and at the end of the experiment for examination by electron microscopy. Effects of the combination between MSO and DCMU on the alga were

examined. the experiments was carried out in 200 ml conical flasks containing 50ml of algal suspension treated with 1 µm of MSO or 10 µm of DCMU or a combination of both chemicals. Untreated algal suspension served as control. Samples were assayed as in the previous experiment.

Effects of light intensities and MSO on the algal rates of 14 CO_2 fixation

Algal suspension treated with 1µm of MSO for 24 was exposed to different light intensities of 100, 300, 500, 1000, 3000, lux and dark respectively in order to study the rates of carbon fixation. The alga was exposed for 30 min. to radioactive sodium bicarbonate (5 µci/ml) at the various intensities. Organic 14 CO_2 fixed cellular and released to the medium was calculated (16).

Effect of MSO on the incorporation of carbon under Ar/O_2/CO_2

The experiment was carried out in 200 ml conical flasks containing 50 ml aliquots of *Nostoc spp*. The alga was treated with 0.5 and 1.0 µm of MSO for 48hr. under a gas mixture of Ar/CO_2 (77.96/22.00/0.4, v/v) with continuous light. Two ml from each treatment were withdrawn and assayed regularly every 12 h for 14 CO_2 fixation after exposure for 30 min to the radioactive sodium bicarbonate organic fixed cellular and released to the medium was again estimated.

Effect of MSO on lichens

A lichen of 1cm in diameter was saturated with a solution of 1.0 µm of MSO for 24 samples were fixed at the beginning and at the end of the experiment for electron microscopy study.

Chemicals

MSO, L-methionine-DL-sulphoximine, sigma ltd., London. DCMU 3-(3,4-dichlorophynile-1,1-dymethel-urea,sigma ltd., London.

Results and discussions

The results presented in this study demonstrate the effects of MSO and DCMU on some physiological activities of the alga *Nostocspp* isolated from the lichen *p. canina*. As shows in figure 1 the reduction of acetylene was more or less unaffected by addition of virus concentration of MSO, while the amount of ammonia released was proportional to the increase in the concentration of the analogue. Only low quantities of ammonia were detected in the untreated algal culture.Ammonia was detected in the medium after six hours of treatment with different concentration of the analogue. These results indicate that newly fixed ammonia is only partly incorporated in to amino acid synthesis in presence of MSO. This is likely due to a partial blocking of the ammoniating pathway in this case the GS – GOGAT system was inhibited, by MSO as shown earlier by (1,3,19) for the blue – green alga *A. cylindrica*, and(20) for Azotobacter. The effect of treatment with MSO on algal growth was shown in Fig.2.The treatment leads to a slight inhibition in the algal growth, starting after six hours as compared to the control. The inhibition in growth may be caused by nitrogen starvation which due to the partial inhibition in the protein synthesis (21). Stewart and rowell(1975)(3) reported a 10% inhibition in vitro in the activity of ammonia assimilating enzymes GS, GOGAT after treatment of the alga *A. cylindrica* with MSO (1µm). Furthermore, electron micrograph of the algal samples treated with MSO for 24hr show a high increases in the number of polyglucoside bodies (PGB), which are considered to be storage bodies of carbon in prokaryotes .Again this increase could be due to inhibition in the ammonia incorporation activity, with a decrease in the protein synthesis leading to a decreases in the carbon consumed by the cells.

Experiment results studying the relation between carbon and nitrogen fixationare confirmed they are dependent (Table 1).

Treatment of the alga with 10μM and 1μM of MSOled to induce in the ammonia release to the medium by about 5 and 10 times respectively higher than the control. However, the ammonia release was found inhibited 50% when the alga was treated with DCMU and MSO together. The result showed that inhibitor blocking the electron transport between Ps 11 and Ps 1, and MSO simultaneously. Furthermore, treatment of the alga with the same concentration of MSO increased the capacity for fixing carbon about three times compared to the control , while it was completely inhibited by DCMU alone, and with DCMU and MSO together (Table 1). The organic carbon released to the medium was less than the control in all treatments, which indicates that there are no effects from MSO or DCMU on the permeability of the algal cell walls (Figure 3). Algal growth was slightly inhibited in all treatments,a greater or complete inhibition in carbon fixation however was happen with DCMU alone (Table.1), this result is agree with that fined by Singh (2011) (12). Electron micrograph show disappearance of the PGB from the algal cells treated with DCMU or DCMU and MSO (Figure 4). The rapid inhibition in carbon fixation of the alga treated with DCMU due to inhibit ATP supply for carbon and nitrogen fixation [22].

Effects of different light intensities 0n the rates of carbon fixation of the alga show thenormal relation between the intensity of light and photosynthetic activity, i.e. the rates of carbon fixation was enhanced gradually with increase in light intensity (Figure 3). Treatment of the alga with 0.5 μM and 1.0 μM of MSO stimulated the carbon fixation rate 5 and 10 times, respectively, compared with the untreated alga. These results confirm the effects of MSO on carbon fixation demonstrated in the previous parts of this study. As is also seen in figure 3 the organic carbon released show no significant differences between treated and untreated alga at the different light intensities used.

Cultivating the alga with and without 1.0 μM MSO under $Ar/O_2 / CO_2$ in absence of N2 gave a reverse relationship between the cellular incorporated carbon and time (Figure 5). Under the incubation condition, less carbon was accumulated when the algae was treated with MSO. The carbon released, however, increased with maximum carbon released being 13% of the total counts after 48 h (Figure 5), for comparative purpose, the lichen *Peltigeracanina*, harboring heterocyst cyanobacteria *Nostocspp* in cephalodia, was treated with MSO. Electron micrograph showed an increase in the PGB over the first hour of treatment, while these disappeared at the end of the experiment (24 h) (Figure 6). The increase in PGB noted over the first hour is probably due to the presence of MSO, leading to increase in the rates of carbon fixation as shown above for free-living algae. However the disappearance of the bodies might be caused by the fungus of the cephalodia consuming MSO at high rates over the experimental time and as a consequence the rates of carbon fixated by the alga will regress to the normal condition that is why with few PGB.

As a conclusion, the acting mechanism system in lichen is not completely similar to the ammonia assimilating inhibitor (MSO), but this is one of theexplanation. Also, there are another factors coming from the physiological intact between the algae and fungus, and the explanation of that is the accumulation of polyglucoside bodies as shown in the electron microscopy study and finally there is a direct physiological relation between Carbon and Nitrogen fixation.

Table.1 Effect of combination between 1 μM of MSO and 10 μM of DCMU on ammonia released, growth and carbon fixation in *Nostocspp*(intercellular and extracellular).

Treatments	nmNH$_3$	Chloro.a μg/ml	CPM of $^{14}CO_2$ fixed (μg chloro.a)$^{-1}$ (ml filtrate)$^{-1}$	
			Intracellular (μgchloro.a)	Extracellular (ml filtrate)
Control	17.50	7.35	1711.00	449.00
1 μM MSO	163.00	7.29	4811.00	314.00
10 μM DCMU	82.00	8.15	3.00	31.00
MSO and DCMU	70.00	6.47	15.00	4.00
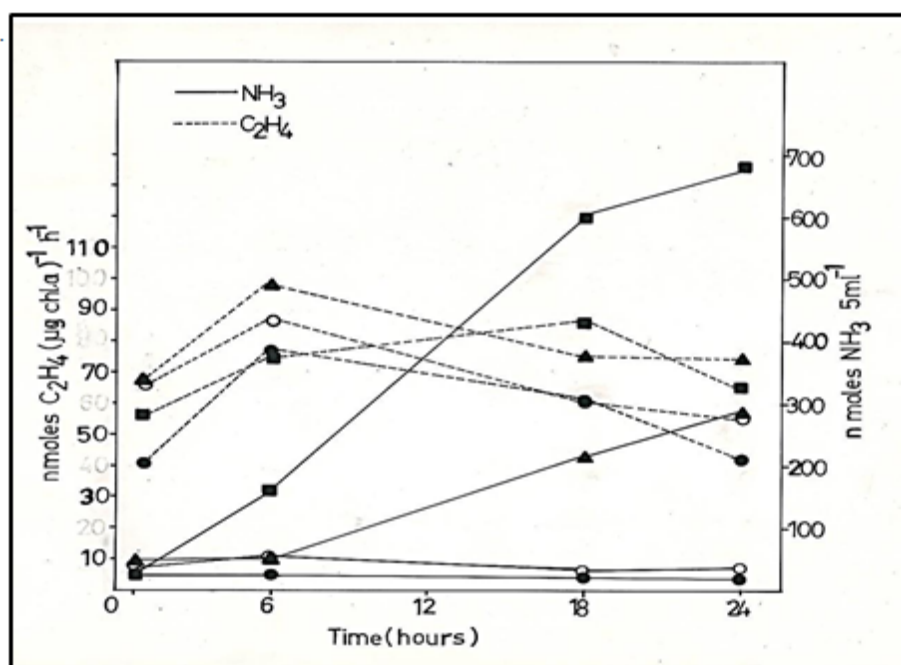
Figure 1. Effect of MSO (0.5μM, 1.0 μM and 2.0 μM) on the nitrogenase activity (C$_2$H$_2$) reduction and ammonia released, 0.5 μM (●), 1.0 μM (▲), 2.0μM (■), controls (○).
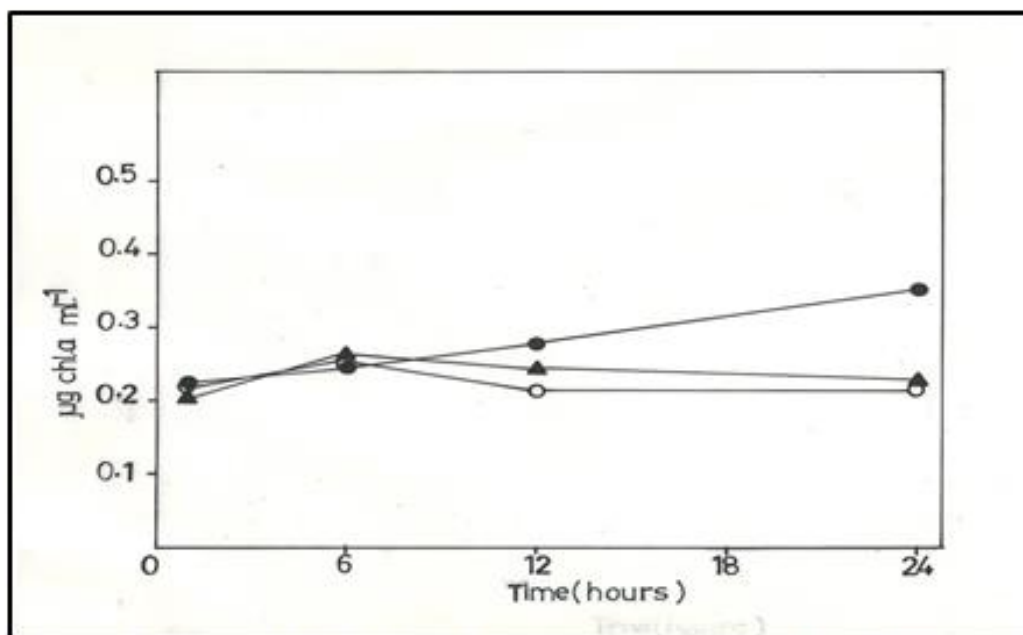
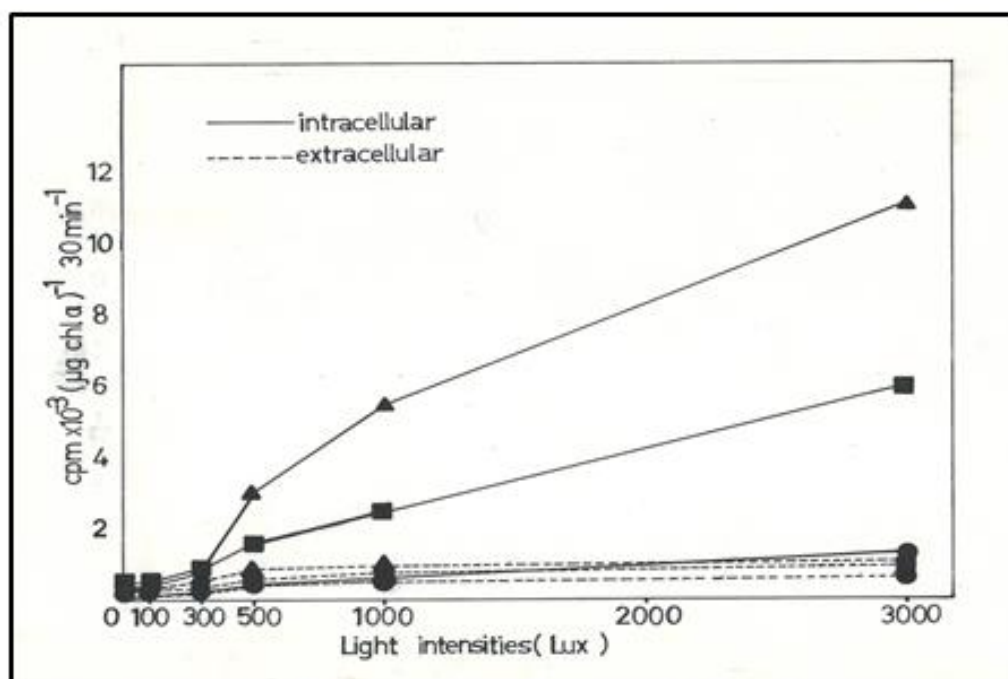Figure 2. Effect of MSO (0.5μM, 1.0 μM) on growth of *Nostoc*spp. controls (●), 0.5 μM (▲), 1.0μM (○).

Figure 3. Effect of Light intensities on the rate of carbon fixation of *Nostoc spp*. treated with 0.5 μM, 1.0 μM of MSO.controls (●), 0.5 μM (■), 1.0μM (▲).
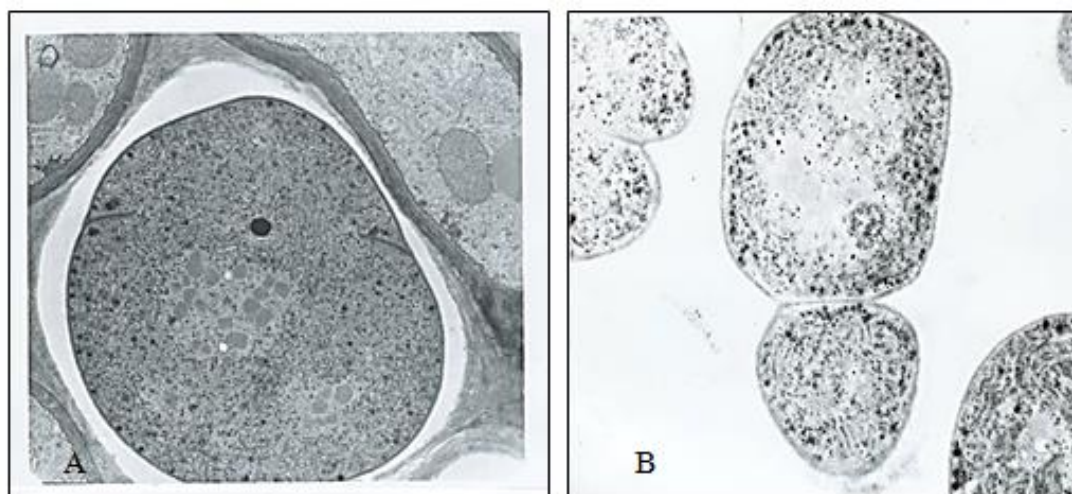
Figure 4. Effects of MSO (0.5μM) on the PGES of the algae *Nostoc spp.*
Electron microscopy 10000 x. A, zero time; B, 24 h.

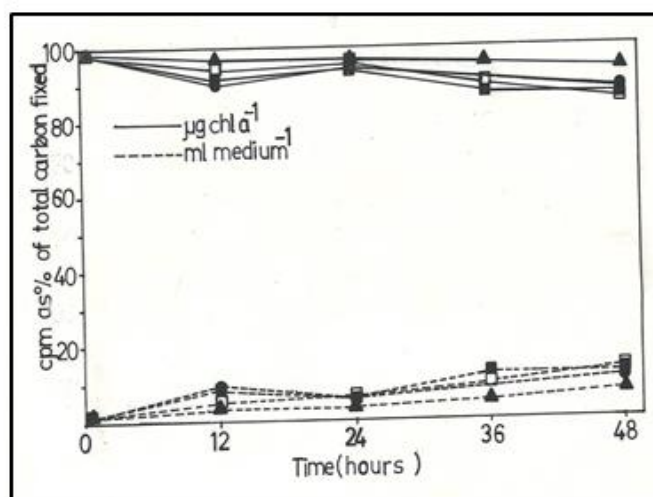Figure 5. Incorporation of $^{14}CO_2$ by the algae *Nostoc spp.* treated with MSO
(0.5 μM, 1.0 μM) cultivation under $Ar/O_2/CO_2$. Control under air (□),
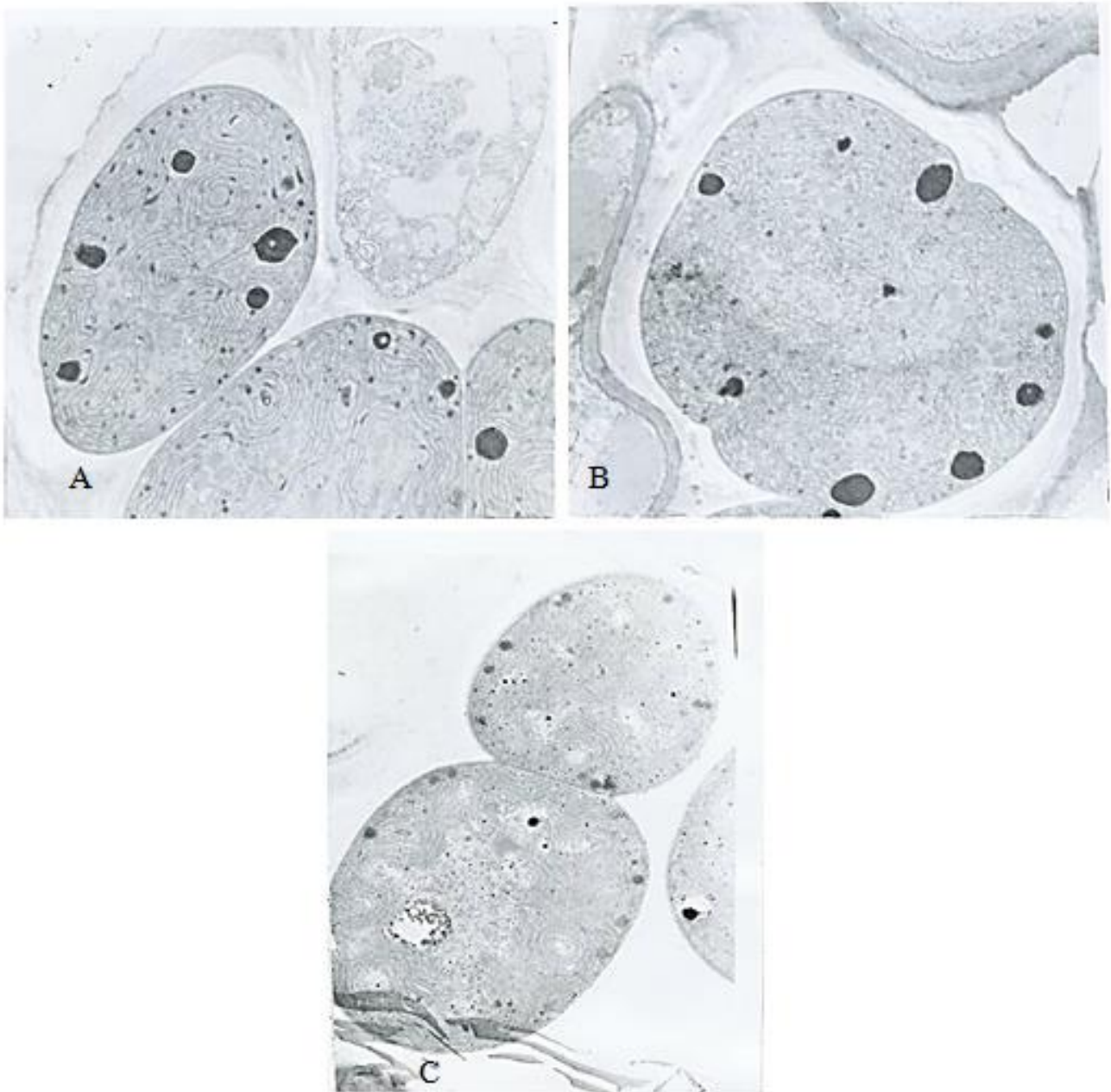control under $Ar/O_2/CO_2$ (●), 0.5μM under$Ar/O_2/CO_2$(▲),1.0μM
under$Ar/O_2/CO_2$(■).

Figure 6.Effects of MSO and DCMU on the PGE numbers of the phycobionta*Nostoc spp*. in the Lichen *P. conina. Electron microscopy 10000x.* A, zero time 1.0 µM (MSO); B, 24 h, Controls C, 0.5 µM MSO+DCMU 24 h.

References

1- Rai, AN, Rowell, P. and Stewart, W. D. P. (1980). NH^+_4 assimilation and nitrogenase regulation in the Lichen *Peltigeraaphthosa*Willd . New phytol. 85:545-555.

2- American Psychological Association (APA). Lichen.(n.d.) the American heritage Science Dictionary. Retrieved October 11, 2015, from Dictionary. Com Website http : /dictionary. Reference. Cam/browse/Lichen.

3- Stewart, W.D.P. and Rowell, P. (1975). Effects of L – methionine – DL- Sulphoximine on the assimilation of newly fixed NH_3, acetylene reduction and heterocyst production in *Anabaena cylindrica*. Biochemical and Biophysical Research Communications. Vol:65,No,3:846-856.

4- Chen, J. Blume, H – P, Beyer, L. (2000). Weathering of rocks induced by Lichen Colonization – a review. Catena, 39:121 – 146 .

5- Ohyama, T. and Kumazawa, K (1980). Nitrogen assimilation in Soybean nodules. II. N_2 assimilation in bacteroidand cytosol fraction of soybean. Soil Sci. Plant Nutr., 26:205 -213.

6- Gomez – Baena, G, Dominguez – Martin, M.A., Donaldson, R. P, Gracia – Fernandaz, J.M and Diez, J.(2015). Glutamine Synthetase sensitivity to oxidative modification during nutrient starvation in *Prochlorococcusmarinus*pcc 9511. Plos one 13:10 (8): eo1 35322. Epub, Aug 13.

7- Jordan, B. R. and Givan, C. V. (1979). Effects of Light and inhibitors on glutamate metabolism in leaf discs of *Viciafaba*., Plant Physiol., 64:1043 -1047.

8- Fries, A.W,Dadsetan, S., Keiding, S., Bak, L. K.,Schousboe, A, w(aagepetersen, H.S., Simonsen, M.,Ott, P., Vilstrup,H. and Sorensen, M. (2014). Effect of glutaminsynthetase inhibition on brain and inter organ ammonia metabolism in bile duct Ligated rats. J .cerebral Blood flow and Metabolism, 34:460 – 466.

9- Dadsetan, S., Kukolj, E., Bak, L.K. , Sorensen, M., Ott, P., Vistrup, H., Schousboe, A., Keiding, S. and waagepetersen, H.S.(2013).Brain alanine formation as an ammonia – Scavenging Pathway during hyperammonemia : Effects of glutamine synthetase inhibition in rats and astrocyte – neuron co – cultures . J. cerebral Blood Flow and metabolism, 33:1235– 1241.

10- Stewart, W.D.P. and Rodgers, G.A. (1977).The Cyanophyte-hepaticsymbiosisII.nitrogen fixation and the interchange of nitrogen and carbon. newphytol., 78:459- 471.

11- Godd, G.A. and Cossar, J.D. (1978) the site of inhibition of photosystem II by 3-(3,4-dicholorophenyl)-N-N-dimethylurea in thylakoieds of the Cyanobacterium*Anabaena cylindrical*. Biochemical and Biophysical Research Communications Vol. 83,No.1,342 -346.

12- Singh,S.,D. Atta,P. and Tirkey, A. (2011) response of multiple herbicide resistant strain of diazotrophiccyanobacterium, *Anabaenavariabilis*, exposed to atrazine and DCMU. Indian J. Experimental Biology, Vol. 49: 298-303.

13- Rowsthoren,S.,Minchin,E.R.,Summerfield,R.J.,Cookson,C, Coombs, J. (1980). Carbon and Nitrogen metabolism in legume root nodules. Phytochemistry, 19:341-355.

14- Allen, M.B., Arnon, D.J. (1955) Studies on nitrogen fixing blue-green algae. I- growth and nitrogen fixation by *Anabaena cylindrical Lemm*. Plant Physiol. 30:366-372.

15- Salorzano, L. (1969). Determination of ammonia in natural water by the phenylhypochloritemethod. Limnology and Occanography, 14:799.

16- Oleary, M.H. (1988). Carbon isotopes in photosynthesis. Bioscience, 38(5):328-336.

17- Mackiney,G. (1941). Absorption of light by chlorophyll solution. J,Biol,Chem.,140:315.

18- Stewart,W.D.P., Fitzgerald,G.P., Burris,R.H. (1968). Acetylene reduction by nitrogen fixing blue-green algae. Arch Microbiol 62:336-348.

19- Rigano, VDIM, Vona, V., Fuggi, A, Rigano,C. (1981) effect of L - methionine–DL-Sulphoximine, a specific inhibitor of glutamine synthetase on ammonium and nitrate metabolism in the unicellular alga *Cylindium caldarium*. Physiol. Plant. 54:47–51.

20- Gordon,J.K., Brill,W.J. (1974). Depression of nitrogenous synthesis in the presence of excess of NH_4Biochem,Biophys Res. Commun., 59:967-971.

21- Ownby, J.D., Shannahan, M., Hood, E. (1979). Protein synthesis and degradation in *Anabaena*during Nitrogen Starvation. J. General microbiol., 110:255-261.

22- Rathnam, C.K.M., Zlinskas, B. (1977). Reversal of 3–(3,4–Dichlorophenyl) –1,1–Dimethylurea inhibition of Carbon dioxide fixation in spinach chloroplast and photoplast by dicarboxylic acid. Plant Physiology. Vol, 50, No. L: 51-53.